Strong Metal-Metal Bonds between *trans*-(amine)$_2$Pt^{II} and -Pd^{II} in Heteronuclear Complexes of Cytosine Nucleobases: Preparation, X-ray Structures, and NMR Spectroscopy†

Michael Krumm,[1a] Ennio Zangrando,[1b] Lucio Randaccio,*[1b] Stephan Menzer,[1a] and Bernhard Lippert*[1a]

Fachbereich Chemie, Universität Dortmund, D-4600 Dortmund, Germany, and Dipartimento di Scienze Chimiche, Università di Trieste, 34127 Trieste, Italy

Received June 20, 1992

trans-[a$_2$Pt(1-MeC-*N3*)$_2$](NO$_3$)$_2$ (a = NH$_3$ (**1a**), CH$_3$NH$_2$ (**1b**); 1-MeC = 1-methylcytosine, C$_5$H$_7$N$_3$O) reacts with K$_2$PdCl$_4$ and *trans*-[(NH$_3$)$_2$Pd(H$_2$O)$_2$](NO$_3$)$_2$ to give *trans*-[a$_2$Pt(1-MeC$^-$-*N3*,*N4*)PdCl]$^+$, PtPdCl (a = NH$_3$ (**2a**); a = CH$_3$NH$_2$ (**2b**)), and *trans*-[a$_2$Pt(1-MeC$^-$-*N3*,*N4*)$_2$Pd(NH$_3$)]$^{2+}$, PtPd(NH$_3$) (a = NH$_3$ (**4a**, **4c**); a = CH$_3$NH$_2$ (**4b**)), respectively, with two 1-methylcytosinato ligands (deprotonated at N4) binding to Pd. The coordination planes of the two d^8 metals are perpendicular to each other, with Pt representing a ligand of Pd and Pd being a fifth ligand of Pt. Displacement of the Cl ligand in **2a** and **2b** by reaction with a stoichiometric amount of AgNO$_3$ yields the corresponding aqua complexes, *trans*-[a$_2$Pt(1-MeC$^-$-*N3*,*N4*)$_2$Pd(H$_2$O)]$^{2+}$, PtPd(H$_2$O) (a = NH$_3$ (**3a**); a = CH$_3$NH$_2$ (**3b**)). PtPd(H$_2$O) has been used as a starting material for the preparation of a large variety of PtPdY compounds with Y = nucleobase such as 1-methylcytosine (**5a**, **5b**), 1-methyluracilate (**6a**, **6b**), 1-methylthyminate (**7a**, **7b**), 9-ethylguanine (**8b**), 9-ethylguaninate (**8a**, **8c**, **8d**), and 2-thiouracil (**14b**), as well as Y = μ-pyrazine (**9b**), 4,4′-bipyridine (**10b**), hexamethylenetetramine (**11b**), SCN$^-$ (**12b**), (CH$_3$)$_2$SO (**13b**), F$^-$ (**15b**), Br$^-$ (**16b**), and I$^-$ (**17b**). Of all ligands Y applied, only Y = thiourea causes instantaneous decomposition of PtPd and re-formation of *trans*-[a$_2$Pt(1-MeC)$_2$]$^{2+}$. Apart from X-ray crystallography, PtPdY compounds are characterized primarily by ^{1}H and ^{195}Pt NMR spectroscopy. The ^{1}H resonances of the bridging 1-MeC$^-$ ligands undergo characteristic upfield shifts as compared to **1a** and **1b** upon Pd binding and deprotonation at the exocyclic amino groups. The Y ligand has a relatively minor effect on the chemical shifts of the 1-MeC$^-$ resonances. Exchange of the axially bound Y and free Y as well as between different coordination sites of Y (linkage isomers of Y = 9-ethylguanine) is slow on the ^{1}H NMR time scale with the nucleobases 1-MeC, 1-MeU, 1-MeT, and 9-EtGH/9-EtG but is fast with 2-thiouracil, pyrazine, 4,4′-bipyridine, hexamethylenetetramine, SCN$^-$, and Me$_2$SO. On the ^{195}Pt NMR time scale, exchange processes in all cases are slow, with individual resonances observable. ^{195}Pt NMR chemical shifts of PtPdY compounds cover a range of 500 ppm, depending on Y, with extremes being OH$^-$ (−2496 ppm) and Me$_2$SO (−1963 ppm). X-ray structures of PtPdY with Y = Cl$^-$ (**2a**), NH$_3$ (**4a**), 1-MeU$^-$ (**6a**), μ-pyz (**9b**), and SCN$^-$ (**12b**) have been performed. Pt–Pd bond lengths are between 2.492(3) Å (**9b**) and 2.521(1) Å (**12b**). The metal-metal bond in these compounds is interpreted in terms of a Pt→Pd donor bond.

Introduction

Among the many fascinating aspects of the chemistry of the antitumor agent *cis*-(NH$_3$)$_2$PtCl$_2$ (*cis*-DDP, Cisplatin),[2] di- and multinuclear complexes with pyrimidine nucleobases and related amidate ligands have attracted particular attention,[3] both for their potential medical application[4] and for their interesting biochemical[5] and chemical properties.[6-10] Considering the broad chemistry that has been developed from *cis*-a$_2$Pt^{II} (a = NH$_3$ or amine) in the last 2 decades, it is rather surprising not to see any analogous chemistry based on the *trans*-a$_2$Pt^{II} isomer. Our early attempts to prepare di- or multinuclear complexes from *trans*-a$_2$PtCl$_2$ and the pyrimidine nucleobases 1-methyluracil (1-MeUH)

† Abbreviations used: 1-MeC = neutral 1-methylcytosine; 1-MeC$^-$ = 1-methylcytosine anion (deprotonated at N4); 1-MeU = 1-methyluracil anion; 1-MeT = 1-methylthymine anion.

(1) (a) Universität Dortmund. (b) Università di Trieste.
(2) (a) Basic chemistry see, e.g.: Lippard, S. J. *Science* **1982**, *218*, 1075. (b) Pt-DNA chemistry see, e.g.: Reedijk, J.; Fichtinger-Schepman, A. M. J.; van Oosterom, A. T.; van de Putte, P. *Struct. Bonding* **1987**, *67*, 53. Eastman, A. *Pharmacol. Ther.* **1987**, *34*, 155. Umapathy, P. *Coord. Chem. Rev.* **1989**, *95*, 129. Johnson, N. P.; Butour, J.-L.; Villani, G.; Wimmer, F. L.; Defais, M.; Pierson, V.; Brabec, V. *Prog. Clin. Biochem. Med.* **1989**, *10*, 1. Sundquist, W. I.; Lippard, S. J. *Coord. Chem. Rev.* **1990**, *100*, 293.
(3) Lippert, B. *Prog. Inorg. Chem.* **1989**, *37*, 1.
(4) (a) Davidson, J. P.; Faber, P. J.; Fischer, R. G., Jr.; Mansy, S.; Peresie, H. J.; Rosenberg, B.; VanCamp, L. *Cancer Chemother. Rep., Part 1* **1975**, *59*, 287. (b) Speer, R. J.; Ridgway, H.; Hall, L. M.; Stewart, D. P.; Howe, K. E.; Lieberman, D. Z.; Newman, A. D.; Hill, J. M. *Cancer Chemother. Rep., Part 1* **1975**, *59*, 629.
(5) (a) Bauer, W.; Gonias, S. L.; Kam, S. K.; Wu, K. C.; Lippard, S. J. *Biochemistry* **1978**, *17*, 1060. (b) Aggarwal, S. K.; Whitehouse, M. W.; Ramachandran, C. In *Cisplatin: Current Status and New Developments*; Prestayko, A. W.; Crooke, S. T.; Carter, S. K.; Eds.; Academic Press: New York, 1980; p 79.
(6) For reviews, see: (a) Lippert, B. In *Handbook of Nucleobase Complexes*; Lusty, J. R.; Ed.; CRC Press: Boca Raton, 1990; Vol. 1, p. 9. (b) Lippert, B. In *Metal-Based Anti-Tumour Drugs*; Gielen, M. F.; Ed.; Freund Publ. House: London, 1988; p 201. (c) Goodgame, M.; Jakubovic, D. A. *Coord. Chem. Rev.* **1987**, *79*, 97. (d) For selected topics, see refs 7-9.
(7) Mixed-valence compounds, see: (a) Barton, J. K.; Szalda, D. J.; Rabinowitz, H. N.; Waszczak, J. V.; Lippard, S. J. *J. Am. Chem. Soc.* **1977**, *99*, 2827; *J. Am. Chem. Soc.* **1979**, *101*, 1434. (b) O'Halloran, T. V.; Mascharak, P. K.; Williams, I. D.; Roberts, M. M.; Lippard, S. J. *Inorg. Chem.* **1987**, *26*, 1261 and references cited. (c) Sakai, K.; Matsumoto, K. *J. Am. Chem. Soc.* **1989**, *111*, 3074. (d) Sakai, K.; Matsumoto, K.; Nishio, K. *Chem. Lett.* **1991**, *1081* and references cited. (e) Trötscher, G.; Micklitz, W.; Schöllhorn, H.; Thewalt, U.; Lippert, B. *Inorg. Chem.* **1990**, *29*, 2541 and references cited.
(8) Diplatinum(III) and tetraplatinum(III) compounds, see: (a) Woollins, J. D.; Kelly, P. F. *Coord. Chem. Rev.* **1985**, *65*, 115. (b) O'Halloran, T. V.; Lippard, S. J. *Isr. J. Chem.* **1985**, *25*, 130. (c) Lippert, B.; Schöllhorn, H.; Thewalt, U. *J. Am. Chem. Soc.* **1986**, *108*, 525. (d) Schöllhorn, H.; Thewalt, U.; Lippert, B. *J. Chem. Soc., Chem. Commun.* **1986**, 258. (e) Lippert, B.; Schöllhorn, H.; Thewalt, U. *Inorg. Chem.* **1986**, *25*, 407. (f) Schöllhorn, H.; Eisenmann, P.; Thewalt, U.; Lippert, B. *Inorg. Chem.* **1986**, *25*, 3384. (g) Hollis, L. S.; Lippard, S. J. *J. Am. Chem. Soc.* **1981**, *103*, 6761. (h) Hollis, L. S., Lippard, S. J. *Inorg. Chem.* **1982**, *21*, 2117. (i) Hollis, L. S.; Roberts, M. M.; Lippard, S. J. *Inorg. Chem.* **1983**, *22*, 3637. (j) Hollis, L. S.; Lippard, S. J. *Inorg. Chem.* **1983**, *22*, 2605. (k) O'Halloran, T. V.; Roberts, M. M.; Lippard, S. J. *Inorg. Chem.* **1986**, *25*, 957. (l) Matsumoto, K.; Harashima, K. *Inorg. Chem.* **1991**, *30*, 3032. (m) Abe, T.; Moriyama, H.; Matsumoto, K. *Inorg. Chem.* **1991**, *30*, 4198. (n) Yamaguchi, T.; Sasaki, Y.; Ito, T. *J. Am. Chem. Soc.* **1990**, *112*, 4038.

0020-1669/93/1332-0700$04.00/0

or 1-methylthymine (1-MeTH), in analogy to the corresponding compounds derived from *cis*-DDP, were largely unsatisfactory, even though in one case a polynuclear, mixed Pt,Ag_2 complex had been isolated and structurally characterized.[11] Our initial suspicion was that the extremely poor solubility of *trans*-a_2PtL_2 (a = NH_3, L = 1-MeU or 1-MeT) precluded any reaction to produce dinuclear complexes of type *trans*-$[a_2PtL_2Pta_2]^{2+}$, but the fact that neither *trans*-$(CH_3NH_2)_2PtL_2$ nor *trans*-$(NH_3)_2Pt(urd)_2$ (urd = uridine), despite their good solubility in water, afforded diplatinum(II) compounds on reaction with *trans*-$[a_2Pt(H_2O)_2]^{2+}$ was in disagreement with this view. Likewise, our attempts to prepare a compound of composition *trans*-$[a_2PtL_2Pta_2]^{2+}$ with L = 1-methylcytosyl, 1-MeC$^-$-*N3,N4*, from the well soluble starting materials *trans*-$[a_2Pt(1\text{-}MeC)_2]^{2+}$ [12] and *trans*-$[a_2Pt(H_2O)_2]^{2+}$/NaOH were unsuccessful, although the corresponding cis isomer (in its head–tail form) had proven to be a thermodynamic sink in the *cis*-a_2Pt^{II}/1-MeC system[13] and the head–head form had been characterized by ^1H NMR spectroscopy in the related enPd^{II} system.[14] It was the observation[15] of a trans→cis isomerization of the ammonia ligands during the reaction of *trans*-$[(NH_3)_2Pd(1\text{-}MeC\text{-}N3)_2]^{2+}$ with *trans*-$[(NH_3)_2Pd(H_2O)_2]^{2+}$ to give the head–tail dinuclear *cis*-$[(NH_3)_2Pd(1\text{-}MeC^-\text{-}N3,N4)_2Pd(NH_3)_2]^{2+}$, which pointed toward a possible steric reason for our failure to prepare *trans*-$[a_2PtL_2Pta_2]^{2+}$ compounds, namely an unfavorable interaction between the trans-positioned NH_3 ligands of two adjacent Pt coordination planes.[16] Subsequent work, carried out to corroborate or disprove this hypothesis, concentrated on possible reactions between the kinetically inert *trans*-$[(NH_3)_2Pt(1\text{-}MeC\text{-}N3)_2]^{2+}$ and highly reactive Pd^{II} species, including *trans*-$[(NH_3)_2Pd(H_2O)_2]^{2+}$. As a result,[17] we isolated and structurally characterized novel dinuclear Pt,Pd 1-methylcytosyl complexes with the two metal coordination planes perpendicular to each other and Pt^{II} formally acting as a ligand of Pd^{II}. Specifically, reaction of *trans*-$[(NH_3)_2Pt(1\text{-}MeC)_2]^{2+}$ with *trans*-$[(NH_3)_2Pd(H_2O)_2]^{2+}$ had yielded a compounds of composition *trans*-$[(NH_3)_2Pt(1\text{-}MeC^-\text{-}N3,N4)_2Pd(NH_3)]^{2+}$ (PtPdY, Y = NH_3), in which the anticipated steric clash between $Pt(NH_3)_2$ and $Pd(NH_3)_2$ entities had been avoided by loss of one of the ammonias of Pd^{II} and a simultaneous orientation of the $Pd(NH_3)$ fragment perpendicular to the Pt plane. While the mutually perpendicular orientation of two d^8 metal ions is not unprecedented (cf. the situation in $[Pt_2(CH_3)_3(Ph_2PCH_2PPh_2)_2]PF_6$ [18] and in $RhPd(Ph_2Ppy_2)(CO)Cl_3$ [19]), our finding appears to be unique with respect to both the extreme shortness of the Pt–Pd bonds and the fact that a similar binding pattern has never been observed in nucleobase coordination chemistry. In all previous cases of Pt,Pd,[9b] Pd,Pd,[20] and Pt_2Pd [9a] nucleobase complexes, the d^8 metal ions had been oriented so as to approach each other via the respective d_{z^2} orbitals, very much as in the case of the pyrophosphito-bridged diplatinum(II) complex or analogous compounds, for example.[21]

Chart I

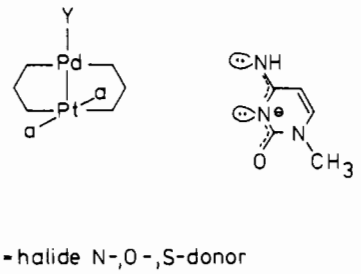

In this report, we extend our previous work[17] on PtPdY compounds to a large variety of derivatives with different Y-ligands (Chart I). Apart from establishing the preparative and structural side of this chemistry, we were particularly interested in any possible effect of different donor ligands (Y = N, O, S) on the Pt–Pd bond and in the behavior of axially bound nucleobases. PtPdY compounds with Y = nucleobase can be considered variants of the well-studied nucleobase complexes of monomeric Pd^{II}.[22] In a future paper,[23] we will report on related heteronuclear complexes containing a *trans*-a_2Pt^{II} entity, two bridging cytosyl nucleobases, and d^{10} metal ions.

Experimental Section

Preparation of Starting Compounds. *trans*-$[(NH_3)_2Pt(1\text{-}MeC)_2](NO_3)_2$ (**1a**) was prepared as reported.[12] *trans*-$[(CH_3NH_2)_2Pt(1\text{-}MeC)_2](NO_3)_2$ (**1b**) was obtained in an analogous way from *trans*-$(CH_3NH_2)_2PtCl_2$,[24] $AgNO_3$, and 1-MeC[25] in 88% yield. Anal. Calcd (found) for $C_{12}H_{24}N_{10}O_8Pt$ (**1b**): C, 22.8 (23.0); H, 3.8 (3.9); N, 22.2 (22.5). *trans*-$[(NH_3)_2Pd(H_2O)_2]^{2+}$ was prepared in situ from *trans*-$(NH_3)_2PdCl_2$ [26] and 2 equiv of a silver salt (H_2O or D_2O, 1 h, 22 °C) and filtration of AgCl.

Preparation of PtPdY Compounds. The subsequently described preparations were not conducted with the aim of optimizing the yields of the various compounds. Crystallization procedures were usually carried out either in a water bath (40 °C) or in a refrigerator with samples covered with Parafilm having small holes. Even with samples of pH > 7, no extra precautions were taken to avoid access of CO_2. Only characteristic IR bands are listed.

trans-$[(NH_3)_2Pt(1\text{-}MeC^-)_2PdCl]NO_3\cdot H_2O$ (**2a**) was obtained from **1a** and K_2PdCl_4 (0.33 mmol each in 50 mL of water, red suspension, pH raised from 3.6 to 8.5 by means of 1 N NaOH, stirred at 22 °C for 20 h in stoppered flask, pH 5.5 then, concentrated to 5-mL volume by rotary evaporation at 30 °C) upon slow evaporation (5 d, 4 °C) as dark, olive-green cubes. Yield 50–60%. Anal. Calcd (found) for $C_{10}H_{20}N_9O_6ClPtPd$: C, 17.2 (17.1); H, 2.9 (3.0); N, 18.0 (18.2); Cl, 5.1 (5.3). IR (cm^{-1}): 2660 s, sp; 1650 vs; 1560 vs; 1340 vs; 795 s, sp; 750 s, sp; 645 s; 515 s; 325 s.

(9) Mixed-metal compounds, see: (a) Micklitz, W.; Müller, G.; Huber, B.; Riede, J.; Rashwan, F.; Heinze, J.; Lippert, B. *J. Am. Chem. Soc.* **1988**, *110*, 7084 and references cited. (b) Micklitz, W.; Riede, J.; Huber, B.; Müller, G.; Lippert, B. *Inorg. Chem.* **1988**, *27*, 1979. (c) Duckworth, D. M.; Goodgame, D. M. L.; Hitchman, M. A.; Lippert, B.; Murray, K. S. *Inorg. Chem.* **1987**, *26*, 1823 and references cited.
(10) Mixed-ligand and mixed-ligand, mixed-metal complexes, see: (a) Micklitz, W.; Renn, O.; Schöllhorn, H.; Thewalt, U.; Lippert, B. *Inorg. Chem.* **1990**, *29*, 1836. (b) Schöllhorn, H.; Thewalt, U.; Lippert, B. *Inorg. Chim. Acta* **1987**, *135*, 155. (c) Lippert, B.; Thewalt, U.; Schöllhorn, H.; Goodgame, D. M. L.; Rollin, R. W. *Inorg. Chem.* **1984**, *23*, 2807.
(11) (a) Dieter, I.; Lippert, B.; Schöllhorn, H.; Thewalt, U. *Z. Naturforsch., B* **1990**, *45*, 731. (b) Schöllhorn, H.; Thewalt, U.; Lippert, B. *J. Chem. Soc., Chem. Commun.* **1984**, *769*.
(12) Lippert, B.; Lock, C. J. L.; Speranzini, R. A. *Inorg. Chem.* **1981**, *20*, 808.
(13) (a) Britten, J. F.; Lippert, B.; Lock, C. J. L.; Pilon, P. *Inorg. Chem.* **1982**, *21*, 1936. (b) Faggiani, R.; Lippert, B.; Lock, C. J. L.; Speranzini, R. A. *J. Am. Chem. Soc.* **1981**, *103*, 1111.
(14) Häring, U. K.; Martin, R. B. *Inorg. Chim. Acta* **1983**, *78*, 259.
(15) Krumm, M.; Mutikainen, I.; Lippert, B. *Inorg. Chem.* **1991**, *30*, 884.
(16) We are aware of a report by Appleton et al., that *trans*-$[a_2Pd(H_2O)_2]^{2+}$ undergoes an isomerization reaction, but this fact by itself does not explain formation of the cis arrangement of both $Pd(NH_3)_2$ entities. cf.: Appleton, T. G.; Hall, J. R.; Ralph, S. F.; Thompson, C. S. M. *Aust. J. Chem.* **1988**, *41*, 1425.
(17) Krumm, M.; Lippert, B.; Randaccio, L.; Zangrando, E. *J. Am. Chem. Soc.* **1991**, *113*, 5129.
(18) (a) Frew, A. A.; Muir-Manojlovic, L.; Muir, K. W. *J. Chem. Soc., Chem. Commun.* **1980**, 624. (b) Brown, M. P.; Copper, S. J.; Frew, A. A.; Muir-Manojlovic, L.; Muir, K. W.; Puddephatt, R. J.; Seddon, K. R.; Thomson, M. A. *Inorg. Chem.* **1981**, *20*, 1500.
(19) Farr, J. P.; Olmstead, M. M.; Balch, A. L. *J. Am. Chem. Soc.* **1980**, *102*, 6654.
(20) Micklitz, W.; Sheldrick, W. S.; Lippert, B. *Inorg. Chem.* **1990**, *29*, 211.
(21) See, e.g.: Roundhill, D. M.; Gray, H. B.; Che, C.-M. *Acc. Chem. Res.* **1989**, *22*, 55 and references cited therein.
(22) (a) Martin, R. B. In *Platinum, Gold, and Other Metal Chemotherapeutic Agents*; Lippard, S. J.; Ed.; ACS Symposium Series 209, American Chemical Society: Washington, DC; 1983; p 231. (b) Breet, E. L. J.; van Eldik, R. *Inorg. Chem.* **1987**, *26*, 2517.
(23) Krumm, M.; Zangrando, E.; Randaccio, L.; Menzer, S.; Danzmann, A.; Holthenrich, D.; Lippert, B. To be submitted for publication.
(24) Arpalahti, J.; Lippert, B.; Schöllhorn, H.; Thewalt, U. *Inorg. Chim. Acta* **1988**, *153*, 45.
(25) Kistenmacher, T. J.; Rossi, M.; Caradonna, J. P.; Marzilli, L. G. *Adv. Mol. Relax. Interact. Processes* **1979**, *15*, 119.
(26) Kauffmann, G. B.; Tsai, J. H. *Inorg. Synth.* **1966**, *8*, 234.

trans-$[(CH_3NH_2)_2Pt(1\text{-}MeC^-)_2PdCl](NO_3)$ (**2b**) was prepared in analogy to **2a** in 69% yield and obtained as dark, olive-green cubes. Anal. Calcd (found) for $C_{12}H_{22}N_9O_5ClPtPd$: C, 20.3 (20.2), H, 3.1 (3.0); N, 17.8 (17.7). IR (cm^{-1}): 3360 s; 3215 s; 1642 vs; 1622 sh; 1558 vs; 1545 vs; 1385 vs; 1330 vs; 805 s; 790 s; 770 s; 635 m; 508 s; 320 s.

trans-$[(NH_3)_2Pt(1\text{-}MeC^-)_2Pd(H_2O)](NO_3)_2$ (**3a**) and *trans*-$[(CH_3NH_2)_2Pt(1\text{-}MeC^-)_2Pd(H_2O)](NO_3)_2$ (**3b**) were prepared in situ from **2a** and **2b**, respectively, upon treatment with 1 equiv of $AgNO_3$ in water (24 h, 22 °C).

trans-$[(NH_3)_2Pt(1\text{-}MeC^-)_2Pd(NH_3)](NO_3)_2\cdot 3H_2O$ (**4a**) was prepared via two routes: (i) **1a** and *trans*-$[(NH_3)_2Pd(H_2O)_2](NO_3)_2$ (1 mmol each in 60 mL of water, pH raised from 3.3 to 8.1 by means of 1 N NaOH, stirred at 22 °C for 20 h, pH at 5 then) were reacted, and the concentrated solution (rotary evaporation to 15 mL) allowed to slowly evaporate at 4 °C. Pure **4a** was obtained as red plates (orange-red after partial loss of water of crystallization) toward the end of the crystallization procedure in ca. 5% yield. From ^1H NMR spectroscopy (cf. Results) it was evident that, although formed in high yield (>60%) initially, **4a** apparently underwent subsequent reactions to other, yet unidentified products. (ii) Alternatively, an aqueous solution of **3a** (0.1 mmol in 25 mL of water) was treated with excess aqueous NH_3 (pH 11) for 2 h at 22 °C. Upon concentration (rotary evaporation, 30 °C) and slow evaporation at 22 °C, **4a** was isolated as a microcrystalline material in 48% yield. Anal. Calcd (found) for $C_{10}H_{27}N_{11}O_{11}PtPd$: C, 15.4 (15.3); H, 3.5 (3.6); N, 19.8 (19.7). IR (cm^{-1}): 1640 vs; 1550 vs; 1380 vs; 810 s; 780 s; 765 s; 640 s; 505 s.

trans-$[(CH_3NH_2)_2Pt(1\text{-}MeC^-)_2Pd(NH_3)](NO_3)_2\cdot 4H_2O$ (**4b**) was prepared in analogy to **4a** from **1b** and *trans*-$[(NH_3)_2Pd(H_2O)_2]^{2+}$ (route i) in 32% yield and isolated as a pale red, microcrystalline material. Anal. Calcd (found) for $C_{12}H_{33}N_{11}O_{12}PtPd$: C, 17.5 (17.4); H, 4.0 (3.7); N, 18.7 (18.6). IR (cm^{-1}): 1640 vs; 1550 vs; 1540 sh; 1385 vs; 810 m; 780 m; 763 m; 637 m; 503 m.

The ClO_4^- salt (3-hydrate), **4c**, was obtained by addition of an excess of $NaClO_4$ to a concentrated, freshly prepared aqueous solution of **4a**. Anal. Calcd (found) for $C_{10}H_{27}N_9O_{13}Cl_2PtPd$: C, 14.1 (14.0); H, 3.2 (3.3); N, 14.8 (14.8). IR (cm^{-1}): 1640 vs; 1500 vs; 1140, 1110, 1090 vs; 760 s; 635 s; 505 m.

trans-$[(NH_3)_2Pt(1\text{-}MeC^-)_2Pd(1\text{-}MeC)]^{2+}$ (**5a**) was prepared on an NMR scale with N3 bound 1-MeC in **5a** identified by its relative signal intensities and its ^1H NMR chemical shifts, which where different from those of free 1-MeC (see Results).

trans-$[(CH_3NH_2)_2Pt(1\text{-}MeC^-)_2Pd(1\text{-}MeC)](ClO_4)_2$ (**5b**) was obtained from **3b** (0.09 mmol in 9 mL of H_2O) and a slight excess of $NaClO_4$. Concentration and slow evaporation of the solution (pH 5.9) yields **5b** as red plates in 82% yield. Anal. Calcd (found) for $C_{17}H_{29}N_{11}O_{11}Cl_2PtPd$: C, 22.3 (21.7); H, 3.2 (3.1); N, 16.8 (16.6). IR (cm^{-1}): 3420 s; 3340 s; 3230 s; 3130 s; 1650 vs; 1565 s; 1540 s; 1510 s; 1310 s; 1100 vs; 800 s; 790 s; 770 s; 640 s; 630 s; 510 m.

trans-$[(NH_3)_2Pt(1\text{-}MeC^-)_2Pd(1\text{-}MeU)]NO_3\cdot 3H_2O$ (**6a**) was prepared as follows: To a solution of **3a** (0.2 mmol in 25 mL of water) was added 1-MeUH (0.25 mmol) and the pH raised from 2.9 to 8.9 (1 N NaOH). The red solution was kept for 2 d at 60 °C, then concentrated to a 6-mL volume (rotary evaporation, 30 °C), and allowed to crystallize at 4 °C. Reddish-brown cubes were isolated in 40% yield after 14 d. Anal. Calcd (found) for $C_{15}H_{29}N_{11}O_{10}PtPd$: C, 21.8 (21.6); H, 3.5 (3.4); N, 18.7 (18.5): IR (cm^{-1}): 3260 vs; 1640 vs; 1560 vs; 1370 s; 1335 s; 815 s; 810 sh; 765 s; 645 s; 500, 510 s.

trans-$[(CH_3NH_2)_2Pt(1\text{-}MeC^-)_2Pd(1\text{-}MeU)]^+$ (**6b**) was obtained from **3b** and a slight excess of 1-MeUH at pD 9 and identified in the ^1H NMR spectrum (relative intensities of resonances as compared to 1-MeC^-; differences in shifts as compared to free ligand 1-MeU/1-MeUH).

trans-$[(NH_3)_2Pt(1\text{-}MeC^-)_2Pd(1\text{-}MeT)]NO_3\cdot 2H_2O$ (**7a**) was obtained in an analogous way as **6a** in 25% yield as reddish-brown cubes. Anal. Calcd (found) for $C_{16}H_{29}N_{11}O_9PtPd$: C, 23.4 (23.7); H, 3.6 (3.7); N, 18.8 (18.5). IR (cm^{-1}): 3430 vs; 3300 vs; 3100 vs; 1650 vs; 1560 vs; 810 s; 770 s; 645 s; 515 m; 475 m.

trans-$[(CH_3NH_2)_2Pt(1\text{-}MeC^-)_2Pd(1\text{-}MeT)]^+$ (**7b**) was again prepared on an ^1H NMR scale and identified on the grounds of relative signal intensities and shift differences relative to the educts.

trans-$[(NH_3)_2Pt(1\text{-}MeC^-)_2Pd(9\text{-}EtG\text{-}N1)]ClO_4\cdot 2H_2O$ (**8a**) was prepared by mixing 9-EtGH (0.5 mmol in 380 mL water) and **3b** (0.5 mmol in 30 mL of water) and adjusting the pH to 10.3 (NaOH). After 22 h at 22 °C (pH 10.2), excess $NaClO_4$ (280 mg) was added, and the solution was concentrated to a 100-mL volume and allowed to very slowly evaporate in a water bath at 40 °C. Microcrystalline, orange **8a** was isolated in 37% yield. Anal. Calcd (found) for $C_{17}H_{30}N_{13}O_9ClPtPd$: C, 22.8 (22.9); H, 3.4 (3.4); N, 20.3 (19.9). IR (cm^{-1}): 1640 vs; 1540 vs; 1490 vs; 1340 s; 1300 s; 1090 vs; 795 s; 775 s; 630 s; 510 m.

trans-$[(CH_3NH_2)_2Pt(1\text{-}MeC^-)_2Pd(9\text{-}EtGH\text{-}N7)](ClO_4)_2$ (**8b**) was prepared in a similar way as **8a**, with no NaOH added, however. The pH at the end of the reaction was 3.5. After concentration to a small volume and addition of excess $NaClO_4$, **8b** was isolated as a red-orange microcrystalline material in 58% yield. Anal. Calcd (found) for $C_{19}H_{31}N_{13}O_{11}Cl_2PtPd$: C, 22.1 (22.0); H, 3.2 (3.2); N, 18.8 (18.6). IR (cm^{-1}): 1700 s; 1640 vs; 1625 sh; 1595 s; 1560 s; 1305 s; 1145 s; 1125 vs; 1090 vs; 805 s; 780 s; 770 s; 640 s; 635 s; 508 s.

The linkage isomer with N1-bound, anionic 9-EtG, **8e**, was identified by ^1H NMR spectroscopy (cf. Results), but not isolated.

trans-$\{[(CH_3NH_2)_2Pt(1\text{-}MeC^-)_2Pd]_2(9\text{-}EtG\text{-}N1,N7)\}(ClO_4)_3\cdot 5H_2O$ (**8c**) was prepared in a similar way as **8a** and **8b**, with a **3b**:9-EtGH ratio of 2:1 and the pH adjusted to 9. To the resulting solution was added an excess of $NaClO_4$; the solution was concentrated initially and then allowed to further evaporate at 40 °C. Orange-red needles of **8c** were isolated in 30% yield. Anal. Calcd (found) for $C_{31}H_{62}N_{21}O_{22}Cl_3Pt_2Pd_2$: C, 20.8 (20.8); H, 3.5 (3.2); N, 16.4 (16.5). IR (cm^{-1}): 3340 s; 1645 vs; 1600 s; 1560 s; 1545 s; 1500 s; 1090 vs; 795 s; 810 sh; 775 s; 640 s; 630 s; 510 m.

trans-$\{[(CH_3NH_2)_2Pt(1\text{-}MeC^-)_2Pd]_2(pyz)\}(NO_3)_4\cdot xH_2O$ (**9b**) was prepared as follows. To a solution of **3b** (0.2 mmol in 40 mL of water) was added pyz (0.1 mmol) and the red solution (pH 3.9) kept at 22 °C for some hours before it was concentrated to a 10-mL volume by rotary evaporation and allowed to crystallize at 22 °C. Reddish-brown cubes of **9b** were isolated in 55% yield after 12 d. Elemental analysis data indicated the presence of 5 molecules of water of crystallization, but X-ray analysis showed only 2 H_2O. Anal. Calcd (found) for $C_{28}H_{58}N_{22}O_{21}Pt_2Pd_2$: C, 20.5 (20.3); H, 3.5 (3.2); N, 18.8 (18.7). IR (cm^{-1}): 1645 vs; 1625 sh; 1570 s; 1560 s; 1390 vs; 790 s; 775 s; 645 m; 515 m.

Reactions of **3b** with 4,4′-bpy (**10b**) and hmta (**11b**) were carried out on NMR scales. Reaction occurs in both cases as evident from the change in color (toward red) and shifting of ^1H NMR resonances of both educts (cf. Results).

trans-$[(CH_3NH_2)_2Pt(1\text{-}MeC^-)_2Pd(SCN)]NO_3\cdot xH_2O$ (**12b**) was prepared by adding KSCN (0.2 mmol) to a solution of **3b** (0.2 mmol in 40 mL of water), concentration to a 10-mL volume by rotary evaporation and slow evaporation in air. **12b** was isolated as green needles in 65% yield. Elemental analysis data indicated the presence of two molecules of water of crystallization rather that one as shown by X-ray analysis. Anal. Calcd (found) for $C_{13}H_{26}N_{10}O_7SPtPd$: C, 20.3 (20.2); H, 3.4 (3.2); N, 18.2 (17.9). IR (cm^{-1}): 2098 s; 1635 vs; 1545 vs; 1535 sh; 1380 vs; 795 s; 765 s; 636 s; 506 m.

Reactions of **3b** with other S-ligands (Me_2SO (**13b**); 2-thiouracil, (**14b**)), with thiourea (complex decomposition), and with halide ions (F^- (**15b**); Br^- (**16b**); I^- (**17b**)) were carried out on NMR scales.

trans-$[(CH_3NH_2)_2Pt(1\text{-}MeC^-)_2Pd(Br)]NO_3$ (**16b**) was also isolated from a solution of **3b** (0.2 mmol in 40 mL of water), to which KBr (0.2 mmol) had been added. Upon slow evaporation of the solution (pH 4.1) in air, yellow-green microcrystals of **16b** were obtained in 42% yield. Anal. Calcd (found) for $C_{12}H_{24}N_9O_6BrPtPd$: C, 18.7 (18.4); H, 2.9 (2.9); N, 16.3 (16.2). IR (cm^{-1}): 3360 s,sp; 3210 s; 1640 vs; 1630 sh; 1550 vs; 1540 sh; 1380 vs; 1330 vs; 800 s; 785 s; 765 vs; 505 s.

A list of all compounds isolated and/or prepared solution is given in Table I.

Instrumentation. IR spectra (KBr pellets) were taken on Perkin-Elmer 580B and Bruker IFs 113v FT spectrometers. UV–vis spectra were recorded on a Perkin-Elmer 555 instrument. The titration of $PtPd(H_2O)$ (**3b**) was carried out by use of an automated titroprocessor (Model 686, Metrohm) and a combination glass electrode. ^1H NMR spectra were recorded on Bruker AM 300 and Bruker AC 200 FT NMR spectrometers using D_2O (with TSP as internal reference), Me_2SO, and MeOD (with TMS as internal standard) as solvents. For aqueous solutions, pD values were determined by use of a glass electrode and addition of 0.4 to the pH meter reader. The 43.02-MHz ^{195}Pt-NMR spectra were recorded on the AC 200 spectrometer at ambient temperature in 5-mm tubes (D_2O, external K_2PtCl_4 reference). Reported shifts are relative to $[PtCl_6]^{2-}$ ($[PtCl_4]^{2-}$: δ, −1630 ppm vs $[PtCl_6]^{2-}$). Typically, 100 000 scans with a sweep width of 100 kHz were acquired. Variable temperature spectra were also run at the AC 200 instrument equipped with a VT-1000 E variable temperature unit. The VT unit was calibrated with samples of methanol or ethylene glycol. Line-shape analyses were performed on an

Table I. List of Compounds Prepared

trans-$[(NH_3)_2Pt(1\text{-}MeC)_2](NO_3)_2$	**1a**
trans-$[(CH_3NH_2)_2Pt(1\text{-}MeC)_2](NO_3)_2$	**1b**
trans-$[(NH_3)_2Pt(1\text{-}MeC^-)_2PdCl]NO_3\cdot H_2O$	**2a**
trans-$[(CH_3NH_2)_2Pt(1\text{-}MeC^-)_2PdCl]NO_3$	**2b**
trans-$[(NH_3)_2Pt(1\text{-}MeC^-)_2Pd(H_2O)]^{2+}$	**3a**[a]
trans-$[(CH_3NH_2)_2Pt(1\text{-}MeC^-)_2Pd(H_2O)]^{2+}$	**3b**[a]
trans-$[(NH_3)_2Pt(1\text{-}MeC^-)_2Pd(NH_3)](NO_3)_2\cdot 3H_2O$	**4a**
trans-$[(CH_3NH_2)_2Pt(1\text{-}MeC^-)_2Pd(NH_3)](NO_3)_2\cdot 4H_2O$	**4b**
trans-$[(NH_3)_2Pt(1\text{-}MeC^-)_2Pd(NH_3)](ClO_4)_2\cdot 3H_2O$	**4c**
trans-$[(NH_3)_2Pt(1\text{-}MeC^-)_2Pd(1\text{-}MeC)]^{2+}$	**5a**[b]
trans-$[(CH_3NH_2)_2Pt(1\text{-}MeC^-)_2Pd(1\text{-}MeC)](ClO_4)_2$	**5b**
trans-$[(NH_3)_2Pt(1\text{-}MeC^-)_2Pd(1\text{-}MeU)]NO_3\cdot 3H_2O$	**6a**
trans-$[(CH_3NH_2)_2Pt(1\text{-}MeC^-)_2Pd(1\text{-}MeU)]^+$	**6b**[b]
trans-$[(NH_3)_2Pt(1\text{-}MeC^-)_2Pd(1\text{-}MeT)]NO_3\cdot 2H_2O$	**7a**
trans-$[(CH_3NH_2)_2Pt(1\text{-}MeC^-)_2Pd(1\text{-}MeT)]^+$	**7b**[b]
trans-$[(NH_3)_2Pt(1\text{-}MeC^-)_2Pd(9\text{-}EtG\text{-}N1)]ClO_4\cdot 2H_2O$	**8a**
trans-$[(CH_3NH_2)_2Pt(1\text{-}MeC^-)_2Pd(9\text{-}EtGH\text{-}N7)](ClO_4)_2$	**8b**
trans-$\{[(CH_3NH_2)_2Pt(1\text{-}MeC^-)_2Pd]_2(9\text{-}EtG\text{-}N1,N7)\}(ClO_4)_3\cdot 5H_2O$	**8c**
trans-$[(CH_3NH_2)_2Pt(1\text{-}MeC^-)_2Pd(9\text{-}EtG\text{-}N1)]^+$	**8d**[b]
trans-$\{[(CH_3NH_2)_2Pt(1\text{-}MeC^-)_2Pd]_2(pyz)\}(NO_3)_4$	**9b**
trans-$[(CH_3NH_2)_2Pt(1\text{-}MeC^-)_2Pd(H_2O)]^{2+}$/4,4′-bpy	**10b**[b]
trans-$[(CH_3NH_2)_2Pt(1\text{-}MeC^-)_2Pd(H_2O)]^{2+}$/hmta	**11b**[b]
trans-$[(CH_3NH_2)_2Pt(1\text{-}MeC^-)_2Pd(SCN)]NO_3\cdot H_2O$	**12b**
trans-$[(CH_3NH_2)_2Pt(1\text{-}MeC^-)_2Pd(H_2O)]^{2+}/(CH_3)_2SO$	**13b**[b]
trans-$[(CH_3NH_2)_2Pt(1\text{-}MeC^-)_2Pd(H_2O)]^{2+}$/2-thiouracil	**14b**[b]
trans-$[(CH_3NH_2)_2Pt(1\text{-}MeC^-)_2PdF]^+$	**15b**[b]
trans-$[(CH_3NH_2)_2Pt(1\text{-}MeC^-)_2PdBr]NO_3\cdot H_2O$	**16b**
trans-$[(CH_3NH_2)_2Pt(1\text{-}MeC^-)_2PdI]^+$	**17b**[b]

[a] Prepared in situ from Cl complex and Ag^+. [b] Not isolated.

AT-IBM PC applying a self-developped program based on the theory of Gutowsky and Holm.[27]

X-ray Crystallography. The following compounds were studied by single-crystal X-ray crystallography: *trans*-$[(NH_3)_2Pt(1\text{-}MeC^-)_2PdCl](NO_3)\cdot H_2O$ (**2a**), *trans*-$[(NH_3)_2Pt(1\text{-}MeC^-)_2Pd(NH_3)](NO_3)_2\cdot 3H_2O$ (**4a**), *trans*-$[(NH_3)_2Pt(1\text{-}MeC^-)_2Pd(1\text{-}MeU)](NO_3)\cdot 3H_2O$ (**6a**), *trans*-$\{[(CH_3NH_2)_2Pt(1\text{-}MeC^-)_2Pd]_2(pyz)\}(NO_3)_4\cdot 2H_2O$ (**9b**), and *trans*-$[(CH_3NH_2)_2Pt(1\text{-}MeC^-)_2Pd(SCN)](NO_3)\cdot H_2O$ (**12b**).

Unit cell dimensions were determined from Weissenberg and precession photographs and refined from 25 reflections in the θ range 13–19° on a CAD-4 Enraf-Nonius single-crystal diffractometer using a graphite-monochromated Mo Kα (λ = 0.7107 Å) radiation. Diffraction data were collected at room temperature. Three standard reflections measured at regular intervals showed no systematic variation in intensity. In all the structures, reflections with $I > 3\sigma(I)$ were corrected for Lorentz–polarization effects, for anomalous dispersion, and for secondary extinction. An absorption correction was applied via an empirical ψ scan to all the structures.

The structures were solved by conventional Patterson and Fourier methods and refined by full-matrix anisotropic least-squares method to the final R and R_w values given in Table II. The relatively high R value in **9b** was due to the poor quality of the available crystals. For compound **12b**, refinement with the signs of *if* ″reversed (or with inverted coordinates) gave R = 0.035 and R_w = 0.038, confirming the correct assignment of absolute configuration.

In all the structures, difference Fourier syntheses revealed the presence of water molecules of crystallization. In **4a**, a site occupancy factor of 0.5 was attributed to OW3 and OW4, on the basis of the peak height in the Fourier map.

The contributions of the hydrogen atoms, which were kept in calculated positions ($B = 1.3B_{eq}$ of the corresponding C- or N-bonded atom), were included in the final refinements. Hydrogen atoms of water oxygens OW1 in **2a** and **12b**, as well as those of OW1–2 in **9b** and OW3–4 in **4a**, were not included in the final refinements. Crystallographic data and details of refinements are reported in Table II.

Atomic scattering factors were as given in ref 28. All calculations were carried out on a MicroVAX2000 computer with the SDP Enraf-Nonius package.[29] Fractional atomic coordinates and equivalent isotropic displacement parameters for **2a**, **4a**, **6a**, **9b**, and **12b** are reported in Tables III–VII. X-ray crystallographic data have been reported in part for **2a**, **4a**, and **6a**.[17]

Selected interatomic distances are listed in Table VIII. Additional data for **9b** and **12b** are given in the supplementary material.

Results

***trans*-$[a_2Pt(1\text{-}MeC)_2]^{2+}$ (a = NH_3, CH_3NH_2).** In aqueous solution, *trans*-$[a_2Pt(1\text{-}MeC)_2]^{2+}$ exists as two rotamers with mutual head–tail and head–head orientations of the two nucleobases. The distribution of the two forms is 3.4:1, with the more abundant rotamer attributed to the head–tail form. Interconversion of the two rotamers are, as with *cis*-$[a_2PtL_2]^{2+}$ (L = cytosine nucleobase),[30] slow on the NMR time scale, even at 85 °C.[31] As a consequence of a field-dependent relaxation mechanism,[32] spectra recorded at 200 or 300 MHz do not display ^4J coupling between the ^{195}Pt isotope and H(5) of 1-MeC as seen in spectra recorded at low field.[33] On the other hand, ^3J coupling of ^{195}Pt with the methyl protons in CH_3NH_2 compounds is usually observed (ca. 40 Hz), in particular after complete H → D isotopic exchange of the amine protons.[34]

Evidence for PtPdY Complex Formation. Reaction of Pd^{II} at the exocyclic amino groups of the cytosine ligands in *trans*-$[a_2PtL_2]^{2+}$ leading to heterodinuclear *trans*-$[a_2Pt(L^-)_2PdY]^{n+}$ (head–head) compounds is evident from ^{1}H NMR, ^{195}Pt NMR, and IR spectra.

In the ^{1}H NMR, considerable upfield shifts of cytosine resonances are observed, which are ca. 0.6–0.7 ppm (H5), 0.5 ppm (H6), and 0.2 ppm (N(1)CH_3) (cf. supplementary material). With both deprotonated exocyclic amino groups binding to Pd^{II} in a head–head fashion, only single sets of 1-MeC$^-$ resonances are observed, unless secondary reactions take place, as found in a few cases (vide infra). Chemical shifts of the 1-MeC$^-$ resonances in PtPdY are subject to slight variations (usually <0.1 ppm), depending on Y (see supplementary material).

PtPdY compounds cover quite a large range of ^{195}Pt chemical shifts (500 ppm). This is surprising considering the fact that manipulations (variations of Y) do not take place in the primary square-planar coordination sphere of Pt^{II}, but rather in the coordination sphere of the fifth ligand (Pd) in the axial position. It is an indication of the strength of the Pt–Pd bond. Due to differences in the time scales of ^{195}Pt and ^{1}H NMR spectra, ligand exchange processes of the type

$$PtPdY + X \rightleftharpoons PtPdX + Y$$

with a given rate constant k in some cases are in the fast exchange limit of the ^{1}H NMR, while they are in the slow exchange limit of the ^{195}Pt NMR. As a consequence, a single, averaged set of resonances is observed in the ^{1}H NMR, but two or, with more complicated equilibria, more resonances are observed in the ^{195}Pt NMR.

In the IR spectra, N3,N4 bridging by 1-MeC$^-$ is evident from characteristic, intense bands at ca. 1650 and 1550 cm^{-1}, as previously observed for dinuclear Pt_2[13a] and Pd_2[15] 1-methylcy-

(27) Gutowsky, H. S.; Holm, C. H. *J. Chem. Phys.* **1956**, *25*, 1228.

(28) *International Tables of Crystallography*; Kynoch: Birmingham, England; 1974; Vol. IV.

(29) Frenz, B. A. Enraf-Nonius Structure Determination Package. Frenz and Associates, College Station, TX, and Enraf-Nonius, Delft, The Netherlands.

(30) Reily, M. D.; Wilkowski, K.; Shinozuka, K.; Marzilli, L. G. *Inorg. Chem.* **1985**, *24*, 37.

(31) Krizanovic, O.; Pesch, F. J.; Lippert, B. *Inorg. Chim. Acta* **1989**, *165*, 145.

(32) Lallemand, J.-Y.; Soulie, J.; Chottard, J.-C. *J. Chem. Soc., Chem. Commun.* **1980**, 438.

(33) See, e.g.: Faggiani, R.; Lippert, B.; Lock, C. J. L. *Inorg. Chem.* **1982**, *21*, 3210.

(34) Pesch, F. J.; Preut, H.; Lippert, B. *Inorg. Chim. Acta* **1990**, *169*, 195.

Table II. Crystallographic Data and Details of Refinement of 2a, 4a, 6a, 9b, 12b for Data Collected at 18 °C Using Mo Kα Radiation (λ = 0.7107 Å)

	2a	4a	6a	9b	12b
formula	$PtPdClO_5N_9C_{10}H_{18}\cdot H_2O$	$PtPdO_8N_{11}C_{10}H_{21}\cdot 3H_2O$	$PtPdO_7N_{11}C_{15}H_{23}\cdot 3H_2O$	$PtPdO_8N_{11}C_{14}H_{24}\cdot 2H_2O$	$PtPdSO_5N_{10}C_{13}H_{22}\cdot H_2O$
fw	699.3	778.9	825.0	811.9	749.9
cryst dimens, mm	0.20 × 0.15 × 0.40	0.20 × 0.20 × 0.60	0.20 × 0.30 × 0.45	0.14 × 0.37 × 0.50	0.10 × 0.35 × 0.55
cryst syst	triclinic	triclinic	triclinic	monoclinic	orthorhombic
space group	$P\bar{1}$	$P\bar{1}$	$P\bar{1}$	$P2_1/c$	$Pca2_1$
a, Å	9.116(4)	7.207(2)	9.956(5)	7.846(3)	14.200(2)
b, Å	10.508(6)	11.692(3)	10.619(6)	10.484(2)	11.497(1)
c, Å	11.370(6)	15.457(4)	14.460(4)	31.069(8)	14.161(5)
α, deg	115.33(2)	108.89(1)	68.66(4)		
β, deg	90.00(3)	101.13(1)	85.88(3)	94.77(2)	
γ, deg	92.62(3)	92.79(1)	67.10(4)		
V, Å^3	983.1(9)	1200.4(5)	1307(1)	2547(2)	2311.9(9)
d(calcd), g cm^{-3}	2.36	2.15	2.09	2.12	2.16
Z	2	2	2	4	4
F(000)	664	752	800	1572	1440
μ(Mo Kα), cm^{-1}	82.7	66.9	61.5	63.1	70.1
2θ max, deg	60	60	56	52	52
% transm: max, min	99.9, 29.7	98.6, 70.5	99.9, 78.8	99.7, 77.9	98.9, 75.6
no. of reflcns measd	5975	7124	6527	5378	2596
no. of indep reflcns with I>3σ(I)	4960	4379	5023	2942	1893
no. of variables	254	317	344	335	289
R	0.038	0.037	0.039	0.080	0.028
R_w	0.048	0.043	0.047	0.115	0.030

Table III. Positional Parameters of Non-Hydrogen Atoms and Thermal Parameters for **2a**

atom	x	y	z	B,[a] Å^2
Pt	0.03316(3)	0.23336(3)	0.17872(3)	2.222(5)
Pd	0.16303(6)	0.35502(6)	0.39691(5)	2.55(1)
O2	–0.2601(7)	0.0957(7)	0.0777(6)	3.6(1)
N1	–0.3867(7)	0.1160(8)	0.2573(6)	3.1(1)
N3	–0.1417(7)	0.2034(7)	0.2726(6)	2.6(1)
N4	–0.0192(8)	0.3106(8)	0.4712(6)	3.3(1)
C1	–0.518(1)	0.043(1)	0.1774(9)	4.0(2)
C2	–0.2635(8)	0.1359(8)	0.1960(7)	2.7(2)
C4	–0.1401(9)	0.2489(8)	0.4044(7)	2.9(2)
C5	–0.272(1)	0.228(1)	0.4638(8)	3.6(2)
C6	–0.390(1)	0.163(1)	0.3884(8)	3.7(2)
O2A	0.1010(7)	0.1806(7)	–0.0922(6)	3.8(1)
N1A	0.3321(8)	0.2698(7)	–0.0861(6)	3.3(1)
N3A	0.2181(7)	0.2770(7)	0.1020(6)	2.6(1)
N4A	0.3326(8)	0.3890(8)	0.3034(6)	3.2(2)
C1A	0.323(1)	0.235(1)	–0.2251(9)	5.0(2)
C2A	0.2120(9)	0.2392(8)	–0.0288(7)	2.8(2)
C4A	0.3378(9)	0.3504(8)	0.1789(7)	2.7(2)
C5A	0.4636(9)	0.3754(9)	0.1144(8)	3.4(2)
C6A	0.457(1)	0.3354(9)	–0.0131(8)	3.5(2)
N11	–0.0560(8)	0.4038(8)	0.1749(7)	3.3(2)
N12	0.1111(7)	0.0523(7)	0.1696(6)	2.9(1)
C1	0.2971(2)	0.4465(3)	0.5907(2)	3.65(5)
N7	0.179(1)	0.680(1)	0.1749(9)	4.9(2)
O71	0.097(1)	0.680(1)	0.2585(8)	7.8(3)
O72	0.181(1)	0.579(1)	0.0675(9)	6.9(3)
O73	0.257(1)	0.786(1)	0.197(1)	12.1(4)
OW1	0.232(2)	0.043(2)	0.414(1)	13.1(6)

[a] Anisotropic refined atoms are given in the form of the isotropic equivalent displacement parameter defined as $(4/3)\sum_i\sum_j a_i a_j \beta(i,j)$.

Table IV. Positional Parameters of Non-Hydrogen Atoms and Thermal Parameters for **4a**

atom	x	y	z	B,[a] Å^2
Pt	0.12383(4)	0.36428(3)	0.24158(2)	2.294(5)
Pd	0.10623(9)	0.35611(5)	0.07584(4)	2.57(1)
O2	0.312(1)	0.5245(6)	0.4285(4)	4.0(1)
N1	0.505(1)	0.6694(7)	0.4087(5)	3.6(2)
N3	0.3054(9)	0.5176(6)	0.2824(4)	2.6(1)
N4	0.277(1)	0.5145(6)	0.1295(5)	3.0(1)
C1	0.583(2)	0.725(1)	0.5105(7)	5.4(3)
C2	0.371(1)	0.5688(7)	0.3756(6)	3.0(2)
C4	0.356(1)	0.5666(7)	0.2192(5)	2.7(2)
C5	0.496(1)	0.6699(8)	0.2551(6)	3.7(2)
C6	0.564(1)	0.7169(8)	0.3471(7)	4.0(2)
O2A	–0.054(1)	0.2178(6)	0.3379(4)	4.0(1)
N1A	–0.219(1)	0.0513(6)	0.2206(6)	4.2(2)
N3A	–0.0552(9)	0.2072(6)	0.1897(5)	2.9(1)
N4A	–0.057(1)	0.1955(6)	0.0374(5)	3.1(2)
C1A	–0.269(2)	–0.002(1)	0.2870(8)	6.1(3)
C2A	–0.109(1)	0.1660(7)	0.2547(5)	2.9(2)
C4A	–0.113(1)	0.1489(8)	0.0941(6)	2.9(2)
C5A	–0.233(1)	0.0350(8)	0.0623(7)	4.0(2)
C6A	–0.282(1)	–0.0091(8)	0.1246(8)	4.5(2)
N11	–0.099(1)	0.4653(6)	0.2518(5)	3.2(2)
N12	0.351(1)	0.2677(6)	0.2346(5)	3.0(1)
N2	0.098(1)	0.3474(7)	–0.0563(5)	3.7(2)
N7	0.219(1)	–0.0393(7)	0.2258(6)	4.2(2)
O71	0.240(1)	–0.0124(7)	0.1564(5)	6.0(2)
O72	0.269(1)	0.0366(8)	0.3041(6)	6.6(2)
O73	0.139(2)	–0.1395(8)	0.2124(7)	7.7(3)
N8	0.575(1)	0.3352(7)	0.0304(5)	3.5(2)
O81	0.679(1)	0.4339(7)	0.0611(6)	5.2(2)
O82	0.542(1)	0.2827(7)	0.0833(5)	6.1(2)
O83	0.504(1)	0.2928(8)	–0.0540(5)	5.7(2)
OW1	0.295(1)	0.6041(6)	0.6181(4)	4.4(2)
OW2	0.981(2)	0.274(1)	0.6826(9)	10.8(4)
OW3	0.307(3)	0.968(1)	0.4629(9)	5.9(4)
OW4	0.980(3)	0.136(2)	0.494(1)	6.5(4)

[a] See footnote *a* in Table III.

tosinato complexes. Only when Y is a nucleobase or a heterocyclic ligand is there some difficulty to readily recognize these bands.

^{1}H NMR Methylamine Resonances of PtPdY. As with the starting compound *trans*-$[(CH_3NH_2)_2Pt(1\text{-}MeC)_2]^{2+}$ (**1b**), ^{195}Pt coupling to the methyl protons is observed even at 200 MHz, ^3J being between 35 and 40 Hz. With few exceptions, e.g. **5b** and **8e** (see below), only singlets (plus ^{195}Pt satellites) are obtained for the two methylamine ligands at ambient temperature in D_2O, once the NH_2–$CH_3 \rightarrow ND_2$–CH_3 isotope exchange is complete. From X-ray data on dinuclear PtMY compounds (M = Pd^{II} or Hg^{II},Ag^I [23]) containing the two trans-oriented CH_3NH_2 groups and/or model building (allowing for free rotation of the NH_2-CH_3 groups about the metal–N bonds), it becomes evident that in principle either an agostic interaction[35] or even hydrogen bonding[36] between the heterometal M and a proton of the methyl groups of CH_3NH_2 could occur (Figure 1). C–Pd and H–Pd distances can be estimated as being ca. 2.9 and 2.1 Å, respectively, when the methyl group is virtually above the Pd in an apical position during the rotation about Pt–N. Metal–H interactions

(35) See, e.g.: (a) Brookhart, M.; Green, M. L. H. *J. Organomet. Chem.* **1980**, *250*, 395. (b) Albinati, A.; Pregosin, P. S.; Wombacher, F. *Inorg. Chem.* **1990**, *29*, 1812. (c) Broderick, W. E.; Kanamori, K.; Willet, R. D.; Legg, J. I. *Inorg. Chem.* **1991**, *30*, 3875.

(36) Brammer, L.; Charnock, J. M.; Goggin, P. L.; Goodfellow, R. J.; Orpen, A. G.; Koetzle, T. F. *J. Chem. Soc., Dalton Trans.* **1991**, 1789.

Table V. Positional Parameters of Non-Hydrogen Atoms and Thermal Parameters for **6a**

atom	*x*	*y*	*z*	B^a, Å^2
Pt	0.20022(3)	–0.05585(3)	0.39748(2)	2.086(5)
Pd	0.25893(6)	–0.12614(6)	0.24654(4)	2.36(1)
O2	0.0875(7)	0.2204(6)	0.4398(4)	3.6(1)
N1	0.0681(8)	0.4015(7)	0.2910(5)	3.0(2)
N3	0.1414(7)	0.1560(6)	0.3054(4)	2.5(1)
N4	0.2041(8)	0.0863(7)	0.1683(5)	3.1(2)
C1	0.033(1)	0.5098(9)	0.3372(7)	4.2(2)
C2	0.0983(8)	0.2562(8)	0.3494(6)	2.7(2)
C4	0.1552(9)	0.1914(8)	0.2039(6)	2.7(2)
C5	0.117(1)	0.3439(9)	0.1451(6)	3.2(2)
C6	0.077(1)	0.4409(9)	0.1885(7)	3.5(2)
O2A	0.2371(7)	–0.2126(6)	0.6166(4)	3.2(1)
N1A	0.3032(8)	–0.4536(7)	0.6397(5)	2.9(2)
N3A	0.2650(7)	–0.2727(6)	0.4785(4)	2.4(1)
N4A	0.3060(8)	–0.3331(6)	0.3383(5)	2.8(1)
C1A	0.303(1)	–0.491(1)	0.7487(6)	3.7(2)
C2A	0.2668(8)	–0.3082(8)	0.5814(5)	2.4(2)
C4A	0.3027(8)	–0.3749(7)	0.4360(5)	2.5(2)
C5A	0.336(1)	–0.5255(8)	0.5005(6)	3.2(2)
C6A	0.3369(9)	–0.5576(8)	0.5999(6)	3.0(2)
N11	–0.0046(8)	–0.0443(7)	0.3811(5)	3.0(2)
N12	0.4025(8)	–0.0630(7)	0.4217(5)	3.2(2)
O29	0.1014(8)	–0.2178(8)	0.1196(5)	5.3(2)
O49	0.5218(8)	–0.1445(8)	0.1207(5)	4.8(2)
N19	0.262(1)	–0.2592(9)	0.0010(6)	5.3(2)
N39	0.3122(9)	–0.1822(7)	0.1229(5)	3.3(2)
C19	0.167(2)	–0.296(1)	–0.0433(9)	8.6(3)
C29	0.218(1)	–0.218(1)	0.0847(6)	4.1(2)
C49	0.441(1)	–0.182(1)	0.0848(7)	4.0(2)
C59	0.478(1)	–0.224(1)	–0.0016(7)	5.1(3)
C69	0.388(1)	–0.261(1)	–0.0369(7)	5.5(3)
N7	0.4309(8)	0.2919(7)	0.2940(5)	3.6(2)
O71	0.476(1)	0.2133(8)	0.2441(6)	7.2(3)
O72	0.4022(9)	0.4229(7)	0.2559(6)	5.4(2)
O73	0.4123(8)	0.2330(7)	0.3833(5)	4.4(2)
OW1	0.3894(9)	0.0816(8)	0.7365(6)	5.4(2)
OW2	0.1913(8)	0.2083(8)	0.9453(5)	5.1(2)
OW3	0.113(1)	0.051(1)	0.7943(7)	8.5(3)

[a] See footnote *a* in Table III.

Table VI. Positional Parameters of Non-Hydrogen Atoms and Thermal Parameters for **9b**

atom	*x*	*y*	*z*	B^a, Å^2
Pt	0.5486(1)	0.1092(1)	0.63691(4)	1.35(2)
Pd	0.5322(3)	0.2707(2)	0.57787(8)	1.76(4)
O2	0.395(3)	–0.145(2)	0.6526(7)	2.7(5)
N1	0.245(4)	–0.196(3)	0.589(1)	2.7(6)
N3	0.383(3)	–0.004(2)	0.5981(8)	1.8(5)
N4	0.377(4)	0.152(3)	0.5432(9)	3.4(7)
C1	0.220(5)	–0.327(4)	0.603(1)	4.2(9)
C2	0.352(4)	–0.112(4)	0.614(1)	2.3(6)
C4	0.334(4)	0.033(4)	0.556(1)	2.8(7)
C5	0.234(6)	–0.051(4)	0.530(1)	3.9(9)
C6	0.193(5)	–0.161(4)	0.547(1)	3.6(8)
O2A	0.725(3)	0.083(2)	0.7257(8)	3.9(6)
N1A	0.878(3)	0.269(3)	0.7353(8)	2.5(5)
N3A	0.712(3)	0.231(3)	0.6713(8)	2.0(5)
N4A	0.691(4)	0.378(2)	0.6161(8)	2.2(5)
C1A	0.922(5)	0.234(4)	0.781(1)	4.2(9)
C2A	0.768(5)	0.190(3)	0.712(1)	2.9(7)
C4A	0.752(5)	0.341(3)	0.656(1)	2.9(7)
C5A	0.879(5)	0.419(3)	0.679(1)	3.0(7)
C6A	0.928(4)	0.378(3)	0.720(1)	2.8(6)
N11	0.744(3)	0.027(3)	0.6082(9)	2.5(6)
C11	0.855(5)	–0.061(4)	0.640(1)	3.7(8)
N12	0.359(3)	0.184(3)	0.6658(9)	2.7(5)
C12	0.303(6)	0.126(5)	0.702(1)	5(1)
N2	0.512(3)	0.410(3)	0.5318(8)	1.8(5)
C21	0.361(4)	0.453(4)	0.517(1)	2.9(7)
C22	0.657(3)	0.450(4)	0.511(1)	3.2(7)
N7	0.028(4)	0.265(2)	0.580(1)	2.7(6)
O71	0.041(3)	0.182(3)	0.6080(9)	4.1(6)
O72	–0.062(5)	0.242(4)	0.5472(9)	7.1(9)
O73	0.104(5)	0.362(3)	0.587(1)	8.2(9)
N8	0.277(4)	0.284(3)	0.430(1)	3.8(7)
O81	0.227(6)	0.360(3)	0.405(2)	10(1)
O82	0.434(4)	0.276(6)	0.428(1)	11(2)
O83	0.225(7)	0.220(6)	0.454(1)	14(2)
OW1	0.597(4)	–0.345(4)	0.681(1)	7(1)
OW2	0.567(5)	–0.063(3)	0.791(1)	8.5(9)

[a] See footnote *a* in Table III.

of these kinds should manifest themselves either in upfield (agostic interaction) or downfield shifts (H bonding) in the ^{1}H NMR. While averaging over three (six) protons (one (two) involved, two (four) others not) would substantially reduce the observable effect on the chemical shift of the CH_3 group anyway, comparison of chemical shifts of this signal in **1b** (2.23 ppm) with PtPdY compounds (e.g. **2b**, 2.55 ppm; **3b**, 2.55 ppm; **4b**, 2.53 ppm; D_2O each) is also hampered by the difficulty in assessing the effect of Pt–Pd bond formation on this resonance. At low temperature (200 K, MeOD) *trans*-$[(CH_3ND_2)_2Pt(1\text{-}MeC^-)_2PdCl]^+$ (**2b**) shows no signs of inequivalent CH_3 resonances that could be interpreted in either way. This may, however, also be due to the fact that rotation of the CH_3 group about the C-N bond is not sufficiently slow as yet to permit two resonances to be observed.

$[PtPdCl]^+$ and $[PtPd(H_2O)]^{2+}$. *trans*-$[a_2Pt(1\text{-}MeC^-)_2PdCl]X$ (a = NH_3, X = NO_3 (**2a**); a = CH_3NH_2, X = NO_3 (**2b**); a = CH_3NH_2, X = Cl (**2c**)) proved excellent starting materials for a large variety of compounds of general formula *trans*-$[a_2Pt(1\text{-}MeC^-)_2PdY]^{n+}$. The IR spectrum of a representative example, **2b**, is deposited in the supplementary material, as are ^{1}H NMR spectra of **2a** and **2b**. From comparison with IR spectra of PtPdY compounds with Y ≠ Cl, the IR band around 320 cm^{-1} is identified as ν(Pd–Cl) in **2a–2c**. Solubility of **2a** in water is good; compounds with methylamine ligand have even better water solubility. **2a** and **2b** are olive-green both in the solid state and in concentrated solution. In dilute aqueous solution, **2a–2c** are yellowish.

The visible spectrum of **2b** in H_2O, pH 5.2, shows two absorptions at 455 nm (474 cm^{-1} M^{-1}) and 575 nm (112 cm^{-1} M^{-1}). Additional intense absorptions are in the UV range, at 232, 268, and ca. 320 nm. Absorptions follow Beer's law, and there is virtually no effect of excess NaCl on the positions of the absorptions in the visible, indicating that Cl^- solvolysis is not significant (see also next paragraph).

From PtPdCl, the corresponding aqua complexes $PtPd(H_2O)$ (**3a**, **3b**) were prepared in situ by use of a silver salt. Like the former, they are of green color with absorptions in the visible spectrum at 433 nm (363 cm^{-1} M^{-1}) and 586 nm (75 cm^{-1} M^{-1}) in the case of **3b** (pH 3.2). Addition of 0.5 equiv of NaCl to an aqueous solution of **3b** (pH 3.2) leads to reformation of the chloro complex **2b**, as evident from ^{195}Pt NMR spectroscopy, which indicates the presence of both aqua species **3b** (–2257 ppm) and chloro species **2b** (–2174 ppm) in an approximately 1:1 ratio. Upon addition of 1 equiv of NaCl per **3b**, **2b** is formed quantitatively, thereby confirming the conclusion drawn from visible spectroscopy. In the ^{1}H NMR spectrum, individual 1-MeC^- resonances for Cl and aqua species are not observed. The requirement for observations of two separate signals, $k < \pi(\Delta\nu)/2^{1/2}$, is not met in the ^{1}H NMR ($\Delta\nu$ for H6 (H5) of 1-MeC^- in PtPdCl and $PtPd(H_2O)$ is 6 Hz (2 Hz)), in contrast to the ^{195}Pt NMR ($\Delta\nu$ = 3570 Hz).

Potentiometric titration of **3b** with NaOH gives a pK_a value of 6.6 for the equilibrium

$$[PtPd(H_2O)]^{2+} \rightleftharpoons [PtPd(OH)]^+ + H^+$$

This value compares with 5.8–7.7 for mononuclear Pd^{II} aqua complexes.[37] The titration curve of **3b** gives some indication (titration of a small amount of a strong acid; consumption of less NaOH than predicted) of μ-OH complex formation according to

$$2[PtPd(H_2O)]^+ \rightleftharpoons [PtPd\text{-}OH\text{-}PdPt]^{3+} + H_3O^+$$

This interpretation is fully confirmed by ^{195}Pt NMR spectroscopy

(37) Lim, M. C.; Martin, R. B. *J. Inorg. Nucl. Chem.* **1976**, *38*, 1911.

Table VII. Positional Parameters of Non-Hydrogen Atoms and Thermal Parameters for **12b**

atom	*x*	*y*	*z*	B^a, Å^2
Pt	0.07844(3)	0.24322(3)	0.250	2.242(6)
Pd	0.09243(6)	0.10981(8)	0.10940(8)	2.53(1)
O2	0.0356(7)	0.4915(8)	0.2842(6)	3.8(2)
N1	0.0132(8)	0.5695(9)	0.1376(8)	3.1(2)
N3	0.0477(7)	0.3717(8)	0.1578(8)	2.6(2)
N4	0.0613(8)	0.248(1)	0.0316(8)	3.7(2)
C1	0.002(1)	0.685(1)	0.177(1)	4.8(4)
C2	0.032(1)	0.476(1)	0.198(1)	3.7(3)
C4	0.048(1)	0.353(1)	0.061(1)	3.1(3)
C5	0.024(1)	0.448(1)	0.003(1)	4.1(3)
C6	0.012(1)	0.554(1)	0.042(1)	4.0(3)
O2A	0.1040(6)	0.2228(8)	0.4585(6)	3.3(2)
N1A	0.1392(8)	0.0338(9)	0.4850(7)	2.7(2)
N3A	0.1103(6)	0.1045(9)	0.3325(7)	2.3(2)
N4A	0.1241(8)	–0.017(1)	0.2027(8)	3.2(2)
C1A	0.145(1)	0.054(1)	0.588(1)	4.3(3)
C2A	0.1170(9)	0.126(1)	0.4272(9)	2.8(2)
C4A	0.1242(8)	–0.003(1)	0.2927(9)	2.7(2)
C5A	0.147(1)	–0.097(1)	0.357(1)	3.3(3)
C6A	0.1520(9)	–0.075(1)	0.449(1)	3.3(3)
N11	–0.0627(6)	0.2100(8)	0.262(1)	3.4(2)
C11	–0.110(1)	0.277(2)	0.337(1)	4.2(3)
N12	0.2187(7)	0.2818(9)	0.243(1)	3.7(2)
C12	0.248(1)	0.376(1)	0.310(1)	4.7(3)
S	0.1092(3)	–0.0211(3)	–0.0111(3)	3.58(7)
N2	0.135(1)	0.107(1)	–0.178(1)	6.1(4)
C3	0.125(1)	0.057(1)	–0.107(1)	3.6(3)
N7	–0.2391(8)	0.311(1)	0.110(1)	4.7(3)
O71	–0.247(1)	0.216(1)	0.149(1)	8.3(4)
O72	–0.166(1)	0.355(2)	0.119(2)	12.6(5)
O73	–0.295(1)	0.361(2)	0.070(2)	18.9(8)
OW1	0.2228(8)	0.383(1)	0.5699(8)	5.6(3)

[a] See footnote *a* in Table III.

Table VIII. Selected Coordination Bond Lengths (Å) and Angles (deg) and Some Relevant Geometric Parameters for Structures 2a, 4a, 6a, 9b, and 12b

	2a x = Cl	**4a** x = NH_3	**6a** X = 1-MeU	**9b** x = pyz	**12b** x = SCN
Pt–Pd	2.518(1)	2.511(1)	2.515(1)	2.492(3)	2.521(1)
Pt–N3	2.005(4)	2.011(4)	2.020(4)	2.07(2)	2.02(1)
Pt–N3A	2.021(4)	2.024(4)	2.020(4)	2.05(2)	2.03(1)
Pt–N11	2.018(5)	2.038(5)	2.021(5)	2.03(3)	2.047(9)
Pt–N12	2.022(5)	2.037(5)	2.036(5)	1.97(3)	2.04(1)
Pd–N4	1.990(5)	2.005(5)	1.985(4)	1.99(3)	1.99(1)
Pd–N4A	1.980(5)	2.014(5)	1.994(4)	2.00(3)	2.02(1)
Pd–X	2.313(1)	2.001(5)	2.056(4)	2.04(3)	2.288(4)
N11–Pt–N12	175.1(2)	178.2(2)	176.2(2)	178(1)	177.2(5)
N3–Pt–N3A	174.2(2)	175.2(2)	174.7(2)	176(1)	174.9(4)
N4–Pd–N4A	173.5(2)	173.1(2)	173.6(2)	175(1)	172.8(4)
Pt–Pd–X	174.03(5)	178.5(2)	178.3(2)	176.7(7)	176.0(1)
α^a	81.6(2)	88.4(2)	87.3(2)	88.3(6)	89.4(3)
β^a	5(2)	9(1)	4.9(6)	6(2)	2(1)
d(N3,N3A)[c]	0.094(6)	0.055(7)	0.082(6)	0.06(2)	1.11(1)
d(N11,N12)[c]	–0.092(7)	–0.042(7)	–0.077(7)	–0.05(2)	–0.10(1)

[a] Angle (deg) between the mean coordination plane of Pd and the mean basal plane of Pt. [b] Angle (deg) between the two 1-MeC$^-$ mean planes. [c] Displacement (Å) of N3, N3A (above) and N11, N12 (below) from the mean coordination PtN_4 plane.

(Figure 2). In addition to the pD-dependent ^{195}Pt NMR shift of the $[PtPd(H_2O)]^{2+}/[PtPd(OH)]^{+}$ couple (–2253 ppm at pD 3.2, –2496 ppm at pD 11), a second, pD-independent ^{195}Pt resonance is observed at pD 6–9, which is assigned to $[PtPd(OH)PtPd]^{3+}$. From ^{1}H NMR spectroscopy it is evident that the 1-MeC$^-$-bridged structure is maintained even at strongly alkaline pD (12.6).

$[PtPd(NH_3)]^{2+}$. Compounds *trans*-$[a_2Pt(1\text{-}MeC^-)_2Pd(NH_3)]^{2+}$ were prepared in two ways, either by reaction of *trans*-$[a_2Pt(1\text{-}MeC)_2]^{2+}$ with *trans*-$[(NH_3)_2Pd(H_2O)_2]^{2+}$ or from $[PtPd(H_2O)]^{2+}$ and NH_4OH. $[PtPd(NH_3)]^{2+}$ compounds are wine red (**4a**) to pale red (**4b**) and are well soluble in water. Absorptions

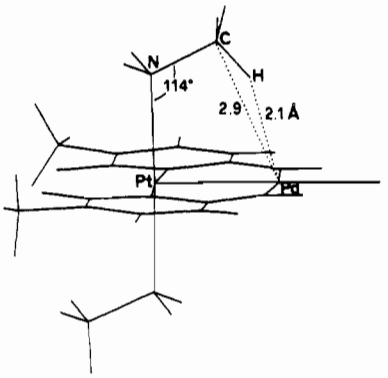

Figure 1. Schematic representation of the orientation of a freely rotating methylamine ligand with a methyl proton in an apical position to Pd. Distances given are taken from idealized models.

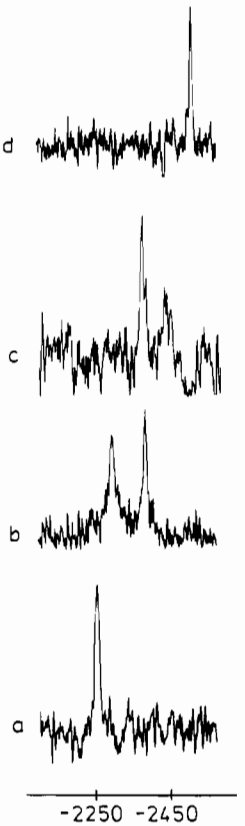

Figure 2. ^{195}Pt NMR spectra (D_2O, ^{1}H decoupled) of $PtPd(H_2O)^{2+}$ (**3b**) at (a) pD 3, (b) pD 6.4, (c) pD 7.3, and (d) pD 11. The ^{195}Pt NMR resonance of the aqua species undergoes a pD-dependent chemical shift from –2253 ppm (pD 3) to –2496 ppm (pD 11) as a consequence of deprotonation to $PtPd(OH)^+$. The pD-independent resonance at –2379 ppm is assigned to the μ-OH species $[PtPd(OH)PdPt]^{3+}$.

of **4b** in the visible are around 400 nm (ca. 380 cm^{-1} M^{-1}) and 508 nm (ca. 110 cm^{-1} M^{-1}). The maxima of these absorptions are somewhat concentration dependent, and addition of excess Cl$^-$ causes the appearance of an absorptions around 450 nm, which we assign to the Cl complex **2b**:

$$[PtPd(NH_3)]^{2+} + Cl^- \rightleftharpoons [PtPdCl]^+ + NH_3$$

The observed raise in pH (7.5–8.6) is consistent with such a substitution reaction.

Peculiarity of *trans*-$[(NH_3)_2Pt(1\text{-}MeC^-)_2PdY]^{2+}$ with Y = H_2O (3a) and Y = NH_3 (4a). Unlike the chloro complex **2a** and the $(CH_3NH_2)_2Pt(1\text{-}MeC^-)_2PtY$ compounds (Y = Cl$^-$, H_2O, NH_3), both **3a** and **4a** have more complicated ^{1}H NMR solution spectra (D_2O). Qualitatively, the spectra of both **3a** and **4a** are similar. Differences with respect to **2a** or **2b**, **3b**, and **4b** refer to additional, minor sets of 1-methylcytosine resonances, which occur at chemical shifts that clearly establish their nature as anionic ligands

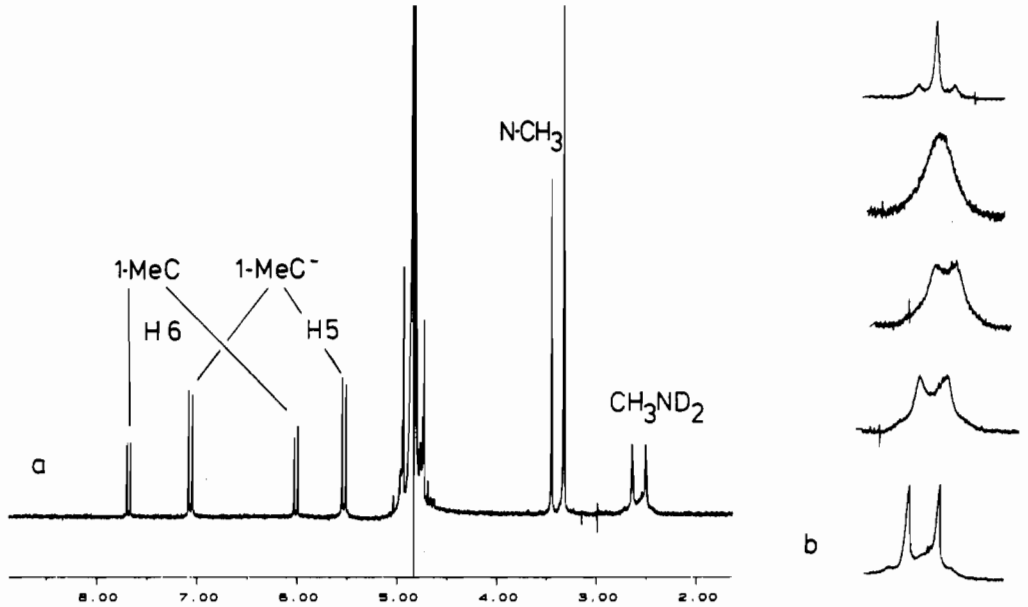

Figure 3. (a) ^{1}H NMR spectrum (D_2O, pD 6.8) of (a) *trans*-$[(CH_3NH_2)_2Pt(1\text{-}MeC^-)_2Pd(1\text{-}MeC)]^{2+}$ (**5b**) at ambient temperature. (b) ^{1}H NMR CH_3ND_2 resonances at 292, 308, 314, 320, and 343 K (bottom to top). Splitting of the methylamine resonance is attributed to hindered rotation of the axial 1-MeC ligand about the Pd–N(3) cytosine bond.

(e.g. **3a**: minor doublets at 7.05, 7.01 ppm (H6), 5.54, 5.40 ppm (H5), and 3.15 ppm (N(1)CH_3)). Work is underway to establish the process(es) causing these spectral features. In the following, mainly complexes with a = CH_3NH_2 will be discussed for this reason.

PtPdY and PtPdYPdPt with Y = N or N,N′ Donor. Apart from the compounds with Y = NH_3, a series of other compounds with N donors has been prepared and studied.

(i) Y = 1-MeC-*N3*. Compounds *trans*-$[(NH_3)_2Pt(1\text{-}MeC^-)_2Pd(1\text{-}MeC)]^{2+}$ (**5a**) and the corresponding CH_3NH_2 analogue **5b** form readily at pH 6 from the respective aqua complexes. Their formation is accompanied by a color change from olive green (aqua species) to dark red (Y = N donor). ^{1}H NMR spectra of **5a** and **5b** display two distinct sets of nucleobase resonances in a 2:1 ratio, corresponding to the bridging anionic and the terminal neutral cytosines. Addition of free 1-MeC to a solution of **5a** or **5b** gives separate ^{1}H NMR signals for axially bound and free 1-MeC. This indicates that any exchange between free 1-MeC and 1-MeC bound to Pd is slow on the ^{1}H NMR time scale. A saturation transfer NMR experiment (D_2O, pD 7.6) carried out at 53 °C with **5b** to which free 1-MeC is added, unambigously confirms that under these conditions, despite two sets of 1-MeC in the ^{1}H NMR spectrum, free and N3-bound 1-MeC are in slow exchange (see supplementary material). Compound **5b** (Figure 3) displays two nonequivalent CH_3 groups (1:1 ratio) of the methylamine ligands in its ^{1}H NMR spectra (D_2O) below ca. 320 K. At this temperature, the two resonances coalesce to a single signal, which sharpens with increasing temperature. This process is fully reversible. Line shape analysis gives activation parameters of $\Delta H^{\ddagger} = 89.2$ kJ mol^{-1} and $\Delta S^{\ddagger} = 68.7$ J K^{-1} mol^{-1}. From model building it becomes evident that the CH_3 groups of CH_3NH_2 can freely rotate above the PtPd-$(N3)_4(N_4)_2$ plane. Thus the nonequivalence of the methylamines must arise from a hindered rotation of the terminal 1-MeC about the Pd–N3 bond, which renders the CH_3 groups to different environments, O2 and N(4)H_2 of the terminal 1-MeC, respectively. The activation parameters compare with rotational barriers $\Delta G^{\ddagger}$ up to 86 kJ mol^{-1} in complexes of type *cis*-$[(amine)_2Pt(nucleobase)_2]^{2+}$, depending on the steric bulk of the amine and the nucleobase.[38] Thus splitting of the methyl resonances of the two CH_3NH_2 groups is a consequence of restricted rotation about another bond, Pd-N3(cytosine).

(ii) Y = 1-MeU-*N3* and 1-MeT-*N3*. Reddish-brown compounds of composition *trans*-$[a_2Pt(1\text{-}MeC^-)_2PdY]^+$ with Y = 1-MeU, a = NH_3 (**6a**) and a = CH_3NH_2 (**6b**) and Y = 1-MeT, a = NH_3 (**7a**) and a = CH_3NH_2 (**7b**) have been identified by ^{1}H NMR spectroscopy and/or have been isolated. As with PtPdY (Y = 1-MeC), the terminal deprotonated 1-MeU and 1-MeT nucleobases are readily recognized by their differences in chemical shifts and intensities relative to the two bridging 1-MeC$^-$ ligands. If rotation of 1-MeU (1-MeT) about Pd–N3 is slow, again a splitting of CH_3 resonances in the methylamine compounds **6b** and **7b** can be expected. The fact that no such splitting is observed could, apart from fast nucleobase rotation, also be explained by the close "similarities" of O4 and O2 oxygens of the terminal 1-MeU (1-MeT). There is no (on the NMR time scale) fast exchange between 1-MeU (1-MeT) and excess free 1-MeUH (1-MeTH) at ambient temperature.

(iii) Y = 9-EtG and 9-EtGH. The following orange to orange-red compounds have been isolated and characterized by elemental analysis and ^{1}H NMR spectroscopy: *trans*-$[(NH_3)_2Pt(1\text{-}MeC^-)_2Pd(9\text{-}EtG\text{-}N1)]ClO_4\cdot 2H_2O$ (**8a**), *trans*-$[(CH_3NH_2)_2Pt(1\text{-}MeC^-)_2Pd(9\text{-}EtGH\text{-}N7)](ClO_4)_2$ (**8b**), and *trans*-$\{[(CH_3NH_2)_2Pt(1\text{-}MeC^-)_2Pd]_2(9\text{-}EtG\text{-}N1,N7)\}(ClO_4)_3\cdot 5H_2O$ (**8c**). In addition, the 9-EtGH-*N1* linkage isomer of the CH_3NH_2 complex (**8d**) has been observed in solution. Identification of the various species is accomplished by means of ^{1}H NMR spectroscopy, specifically the chemical shift of the H8 resonance of 9-ethylguanine and its intensity relative to the 1-MeC$^-$ resonances. Consistent with data on guanine complexes of Pt^{II},H8 resonances of 9-EtGH-*N7* occur downfield relative to the free 9-EtGH, while those of 9-EtG-*N1* are upfield,[39,40] and, as expected, formation of 9-EtGH-*N7* compounds is favored at low pH, while 9-EtG-*N1* compounds were obtained at pH 10. The pK_a of the guanine N(1)H, as determined by potentiometric titration of **8b**, was found to be 8.8, thus close to, albeit somewhat higher than, values found

(38) (a) Cramer, R. E.; Dahlstrom, P. L. *J. Am. Chem. Soc.* **1979**, *101*, 3679. (b) Cramer, R. E.; Dahlstrom, P. L.; Seu, M. J. T.; Norton, T.; Kashiwagi, M. *Inorg. Chem.* **1980**, *19*, 148. (c) Reily, M. D.; Marzilli, L. G. *J. Am. Chem. Soc.* **1986**, *108*, 6785. (d) Hambley, T. W. *Inorg. Chem.* **1988**, *27*, 1073.

(39) (a) Raudaschl-Sieber, G.; Schöllhorn, H.; Thewalt, U.; Lippert, B. *J. Am. Chem. Soc.* **1985**, *107*, 3591. (b) Frommer, G.; Schöllhorn, H.; Thewalt, U.; Lippert, B. *Inorg. Chem.* **1990**, *29*, 1417. (c) Frommer, G.; Mutikainen, I.; Pesch, F. J.; Hillgeris, E. C.; Preut, H.; Lippert, B *Inorg. Chem.* **1992**, *31*, 2429.

(40) van der Veer, J. L.; van den Elst, H.; Reedijk, J. *Inorg. Chem.* **1987**, *26*, 1536.

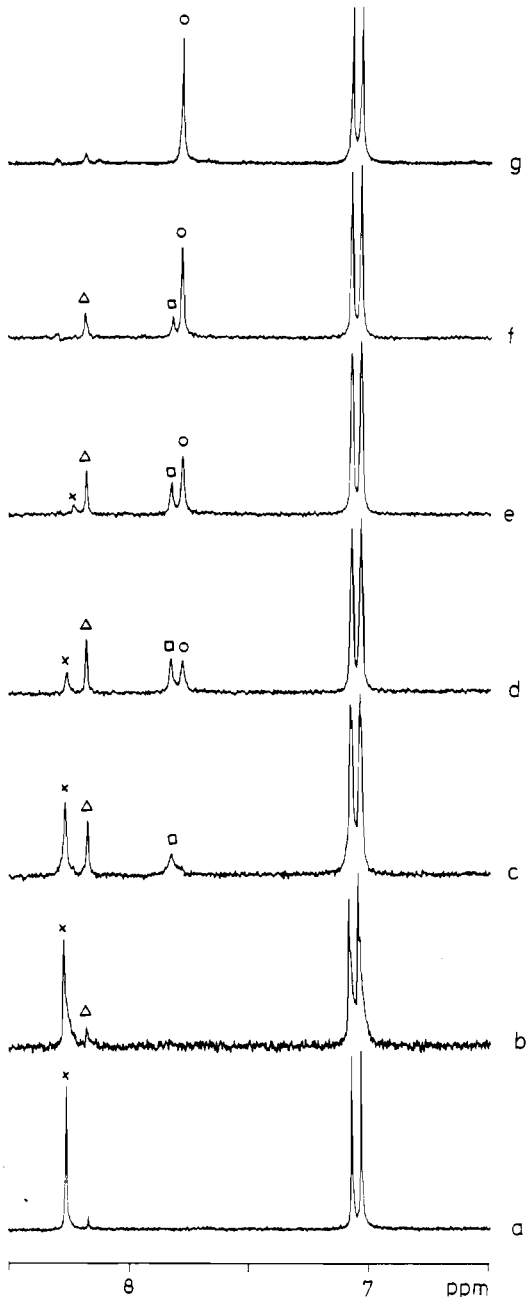

Figure 4. ^{1}H NMR spectra (D_2O, aromatic region only) of PtPd(9-EtGH-*N7*)$^{2+}$ (**8b**) at (a) pD 5.2, (b) pD 6.1, (c) pD 7.0, (d) pD 7.9, (e) pD 8.5, (f) pD 9.2, and (g) pD 10.0. The assignment of the 9-ethylguanine H8 resonances is as follows: (×) 9-EtGH-*N7* species (**8b**); (△) 9-EtG-*N1*,*N7* species (**8c**); (○) 9-EtG-*N1* species (**8d**); (□) free 9-EtGH. The reverse process (with **8d** as starting compound) has also been studied and proceeds via the same intermediates.

in Pt^{II} complexes.[41] Several ^{1}H NMR spectroscopic features of the various complexes deserve mentioning: First, the CH_3NH_2 resonance of the N1 bound isomer **8d** is split in two signals with a 1:1 ratio, as with the Y = 1-MeC compound **5b**. Considering the similarity of guanine-N1 to cytosine-N3, this fact is not surprising. In the N7 isomer **8b**, a single resonance for the two CH_3NH_2 groups is observed. Second, in the N7,N1-bridged 9-EtG complex **8c**, both types of CH_3NH_2 resonances are observed. In addition, the H5 resonances of the bridging 1-MeC$^-$ ligands are clearly split in a 1:1 ratio due to the inequivalence of N1- and N7-bound PtPd. Third, starting out from the (9-EtG-*N1*) isomer **8d** (pD 10.1) and lowering the pD to 4.9 lead to a complete linkage isomerism to give the (9-EtGH-*N7*) isomer **8b**. This process, which is fully reversible (Figure 4), proceeds via the dinuclear (9-EtG-*N1*,*N7*) complex **8c** and free 9-EtGH/9-EtG according to

$$2\text{PtPd(9-EtG-}N1\text{)} + \text{H}^+ \rightleftharpoons \text{PtPd(9-EtG-}N1,N7\text{)PdPt} + \text{9-EtGH}$$

and

$$\text{PtPd(9-EtG-}N1,N7\text{)PdPt} + \text{9-EtGH} + \text{H}^+ \rightleftharpoons 2\text{PtPd(9-EtGH-}N7\text{)}$$

This reaction sequence, which is evident from ^{1}H NMR changes in guanine-H8 resonances, is different from that proposed for the migration of (dien)Pt^{II} from N1 to N7 of guanine, according to which passage of the metal ion occurs intramolecularily without going through a dinuclear intermediate.[41] The reverse process, migration of (dien)Pt^{II} and (dien)Pd^{II} from N7 to N1 of inosine, has been reported to also occur via a dinuclear N1,N7 complex and free nucleobase as in our case.[42]

(iv) Bridging Di- and Tetraamines. Pyrazine (pyz)[43] and 4,4′-bipyridine (4,4′-bpy)[44] are bridging ligands frequently used in inorganic chemistry. Coordination of pyz and 4,4′-bpy to PtPd(H_2O) with substitution of the aqua ligand is evident from the rapid change in color (green to red) and the fact that the bpy ligand rapidly dissolves in water in the presence of PtPd(H_2O). The μ-pyz complex *trans*-{[$(CH_3NH_2)_2$Pt(1-MeC$^-$)$_2$Pd]$_2$(μ-pyz)}$^{4+}$ (**9b**) has been isolated as its nitrate salt and structurally characterized. In the ^{1}H NMR spectrum, the four pyrazine protons of **9b** show up as a broad singlet at 8.79 ppm (D_2O, pD 5). The Pd–N(pyz) bonds are labile on the ^{1}H NMR time scale, as seen from signal averaging of the pyz resonances when the (pyz):(PtPd) ratio is varied from 2:1 to 1:2. In the ^{195}Pt NMR, resonances of the aqua complex (–2253 ppm), of PtPd(μ-pyz)-PdPt (**9b**) (–2256 ppm), and of PtPd(pyz) (–2256 ppm) are not resolved individually, but the color change and the effect seen in the ^{1}H NMR spectrum are fully consistent with displacement of Y = H_2O by Y = N(pyz).

The 4,4′-bpy resonances (7.73 and 8.61 ppm, d, 6.1 Hz; D_2O, pD 8) are shifted downfield in the presence of PtPd(H_2O), e.g. by 0.30 ppm and 0.16 ppm, respectively, at a (4,4′-bpy):(PtPd) ratio of 1:2 (pD 5). According to ^{195}Pt NMR spectroscopy, PtPd(μ-4,4′-bpy)PdPt is formed quantitatively under these conditions (–2231 ppm). With increasing r,[45] a second resonance appears at –2320 ppm, which is the only one at $r \geq 1.5$ and is therefore assigned to PtPd(4,4′-bpy).

We have also added hexamethylenetetramine (hmta, $C_6H_{12}N_4$) to PtPd(D_2O) in D_2O and observed a color change from green to orange-red, indicative of Pd coordination to one or more amino nitrogens. The CH_2 signal in the ^{1}H NMR is a moderately broad singlet (half width 15 Hz at 300 K) with indications of some fine structure at ca. 4.95 ppm ((hmata):(PtPd) = 1:1, pD 5). The corresponding ^{195}Pt NMR resonance occurs at –2214 ppm. Increasing r and the pD does not cause a shift of this resonance (e.g. r = 2, pD 9, –2213 ppm). It therefore is assigned to the 1:1 complex **11b**. At r = 0.5, pD 4.6 only a single ^{195}Pt resonance is observed at –2205 ppm, yet no resonance due to PtPd(D_2O) is seen. Below pD 4 the H^+ successfully competes for binding to N sites of hmta as seen by the appearance of a ^{195}Pt resonance due to PtPd(D_2O). Unlike in the hmta/Cu system,[46] an analytically pure compound of hmta with PtPd was not obtained.

(41) See, e.g.: Faggiani, R.; Lippert, B.; Lock, C. J. L.; Speranzini, R. A. *Inorg. Chem.* **1982**, *21*, 3216.

(42) Scheller, K.; Scheller-Krattiger, V.; Martin, R. B. *J. Am. Chem. Soc.* **1981**, *103*, 6833.

(43) See, e.g.: (a) Creutz, C.; Taube, H. *J. Am. Chem. Soc.* **1969**, *91*, 3988. (b) Gross, R.; Kaim, W. *Inorg. Chem.* **1986**, *25*, 498. (c) Haynes, J. S.; Kostikas, A.; Sams, J. R.; Simopoulos, A.; Thompson, R. C. *Inorg. Chem.* **1987**, *26*, 2630. (d) Lay, P. A.; Magnuson, R. H.; Taube, H. *Inorg. Chem.* **1988**, *27*, 2364 and references cited.

(44) Neyhart, G. A.; Meyer, T. J. *Inorg. Chem.* **1986**, *25*, 4808.

(45) r defined as ratio between ligand and PtPd.

(46) Stocker, F. B. *Inorg. Chem.* **1991**, *30*, 1472.

PtPdY with Y = S Donor. Reactions of $PtPd(H_2O)$ with a variety of S-containing molecules have been performed and followed by ^1H and ^{195}Pt NMR spectroscopy.

(i) Y = SCN. *trans*-$[(CH_3NH_2)_2Pt(1\text{-}MeC^-)_2Pd(SCN)]NO_3\cdot H_2O$ (**12b**) has been isolated and structurally characterized. In the solid state, S coordination has been confirmed. The ^{195}Pt NMR resonance of **12b** in water at −2080 ppm is assigned to this complex with both S and N coordinating to Pd.[47] This binding pattern is not uncommon for Pd compounds.[48] In the ^1H NMR spectra of **12b** or mixtures of **3b** and SCN (pD 3.6–4.3) only averaged 1-MeC^- resonances are observed. There are no signs of complex decomposition up to at least pD 10.

(ii) Y = Me_2SO. A color change from green to red upon addition of Me_2SO to an aqueous solution of **3b** (pD ≈ 3.1) indicates coordination of Me_2SO. According to ^1H NMR spectroscopy (varying r),[45] the compound(s) formed is(are) labile. Even in the presence of a large excess of Me_2SO over PtPd, there is no sign of decomposition of the PtPd entity. Observed ^{195}Pt NMR chemical shifts depend upon r:[45] with r = 0.5, a single resonance is observed at −2253 ppm, with r = 1, two resonances at −2257 and −1963 ppm are observed, and with r = 3, a single resonance at −1966 ppm is observed. The resonance at −2253 ± 2 ppm could be either due to the starting complex and/or an O-bound species, while the −1966 ppm resonance is tentatively assigned to a S-bound complex **13b**.

(iii) Y = 2-Thiouracil. Mixtures of **3b** and 2-thiouracil (2-SUH_2) (r = 1, D_2O, pD 1.8–4.5) give single sets of resonances both for 1-MeC^- ligands and the aromatic protons of 2-thiouracil. Compared to the starting compounds, ^1H NMR resonances are shifted downfield (2-SUH_2: H5, ca. 0.3 ppm; H6, ca. 0.05 ppm at pD ≈ 2). Addition of base (e.g. pD 8.5) results in complete decomposition to *trans*-$[a_2Pt(1\text{-}MeC)_2]^{2+}$, with Pd^{2+} precipitating as a 2-thiouracilato compound not further characterized. ^{195}Pt NMR spectra reveal several signals of intact PtPdY, depending on the pD. With r = 1, pD 1.8, a single ^{195}Pt resonance is seen at −2076 ppm, which is assigned to an S-bound neutral 2-thiouracil (compound **14b**). This resonance undergoes some shift as the pD increases (pD 2.8, −2083 ppm; pD 3.6, −2102 ppm; pD 4.5, −2129 ppm), probably as a result of the beginning of ligand deprotonation (pK_{a1} unmetalated 2-thiouracil is ca. 7.75). At pD 3.6, a new resonance grows in at −2125 ppm, and at pD 4.5 three resonances are seen, at −2129, −2148, and −2340 ppm with relative intensities of 4:3:3. The latter resonance is in the shift range typical of PtPdY and Y = N donor. We cannot, at present, assign the third ^{195}Pt resonance.

(iv) Y = Thiourea. Addition of thiourea, tu (r = 1-2), to **3b** leads to complete decomposition of **3b** according to

$$\textit{trans}\text{-}[a_2Pt(1\text{-}MeC^-)_2Pd(H_2O)]^{2+} + n\text{tu} + H_2O \rightleftharpoons \textit{trans}\text{-}[a_2Pt(1\text{-}MeC)_2]^{2+} + [Pd(tu)_n]^{2+} + 2OH^-$$

as seen from ^1H NMR spectroscopy and evident from the rise in pH.

PtPdY with Y = Halogen. Addition of excess halide (F^-, Br^-, I^-) to aqueous solutions of **3b** results in formation of the respective halide complexes **15b**, **16b**, and **17b**. ^{195}Pt NMR shifts are −2342 ppm (Y = F^-), −2099 ppm (Y = Br^-), and −2000 ppm (Y = I^-). The bromide complex **16b** has been isolated.

X-ray Crystallography: Cation Structures. The ORTEP drawing of the cation of **6a** is shown in Figure 5. The numbering scheme applies also to **2a** and **4a**, substituting the 1-MeU ligand by Cl and NH_3 (N2), respectively. The ORTEP drawings of **9b** and **12b** are given in Figure 6 and 7, respectively.

The Pt and Pd atoms are bridged by two almost parallel 1-MeC^- ligands, trans coordinated to Pt through N3 and N3A in a head–head arrangement. Pd is surrounded by two deprotonated amino groups (N4), Y, and Pt, so that all the cations have a very similar

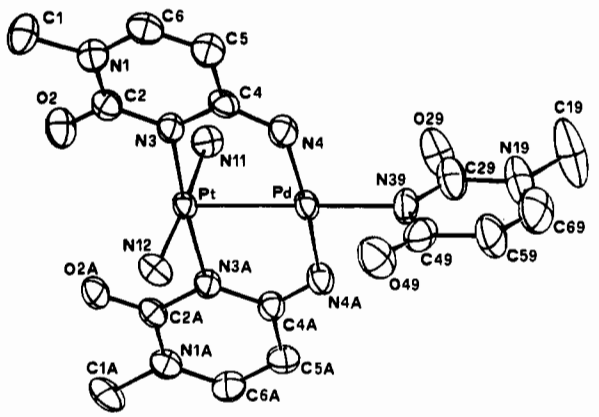

Figure 5. ORTEP drawing and atom numbering scheme of the cation of **6a** (50% probability thermal ellipsoids). The same scheme applies to cations of **2a** and **4a** by substituting N39 with Cl and N2, respectively.

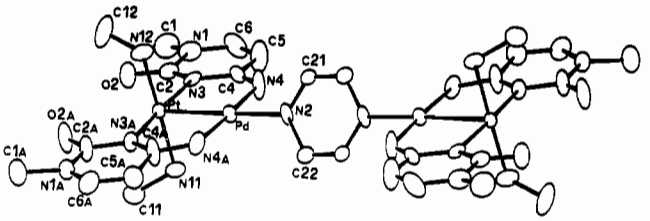

Figure 6. ORTEP drawing and atom numbering scheme of the cation of **9b** (50% probability thermal ellipsoids). The numbering scheme refers to atoms of the crystallographic independent moiety.

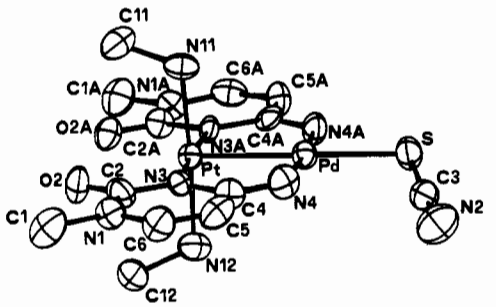

Figure 7. ORTEP drawing and atom numbering scheme of the cation of **12b** (50% probability thermal ellipsoids).

$a_2Pt(1\text{-}MeC^-)_2Pd$ moiety. Therefore the cations are characterized by an essentially square planar coordination around Pd and a square pyramidal one around Pt with Pd in the apical position (Figures 5–7). In **9a** two of the above units are bridged by the bidentate pyz ligand to give the tetranuclear cation of Figure 6, which possesses a crystallographic symmetry center. The Pd coordination plane and the Pt basal plane are nearly perpendicular with interplanar angles ranging from 81.6(2) to 89.4(3)° (Table VIII, α angle). The interplanar angles between the two 1-methylcytosinato groups vary from 2(1) to 9(1)° (Table VIII, β angle). In **6a**, 1-MeU is coordinated through N39 and its molecular plane is almost perpendicular to the Pd coordination plane (75.1(2)°). The planar pyz ligand is **9b** and the essentially planar PdSCN fragment in **12b** make dihedral angles of 59(2) and of 18.6(3)°, with their respective Pd coordination planes.

Some selected bond lengths and angles are reported in Table VIII. Since the structure determination of **9b** is of low accuracy (see Experimental Section), in the following discussion its bond lengths and angles are not taken into account, except for the metal–metal distance.

The Pt–Pd distances of the cations are very similar, ranging from 2.492(3) (Y = pyz) to 2.521(1) Å (Y = SCN). When Y = N ligand, the intermetallic distances are in the lower part of the range. The Pt–N11 and Pt–N12 distances exhibit some variability but do not differ more than 0.02 Å in NH_3 derivatives, but they appear slightly longer *in* **12b**.

(47) For r = 0.3, an additional resonance due to **12b** is observed.
(48) Norbury, A. H. *Adv. Inorg. Chem. Radiochem.* **1975**, *17*, 232.

The Pd-Cl distance of 2.313(1) Å in **2a** is intermediate between that of 2.298(1) Å reported in *trans*-$PdCl_2(1\text{-}MeC)_2$[49] and that of 2.374(2) Å reported in a PdCl complex with a $(Ph)_3P$ ligand trans to Cl.[50]

The Pd-NH_3 distance of 2.001(5) Å in **4a** is shorter than that of 2.039(3) Å reported[15] in *trans*-$[Pd(NH_3)_2(1\text{-}MeC)_2]^{2+}$ and of the mean value of 2.042(2) Å found in *cis*-$[(NH_3)_2Pd(1\text{-}MeC^-)_2Pd(NH_3)_2]^{2+}$.[51] The Pd-(1-MeU) distance is 2.056(4) Å, whereas the Pd-S distance is 2.288(4) Å, very close to that of 2.293(3) Å found in $[Pd_2(4\text{-}mpyt)_4]$, where a N atom is trans to S, but shorter than that of 2.336(1) Å found in $[Pd(mpytH)_4]Cl_2$ (mpytH = 4-methylpyridine-2-thiolate).[52] The above comparison shows that the Pd–Y bond is scarcely affected by the trans influence of the Pt atom.

The almost planar Pt(N3–C4–N4)$_2$Pd moiety is slightly bowed at the Pt and Pd centers, as shown by the N3–Pt–N3A and N4–Pd–N4A angles given in Table VIII. Such distortion slightly affects the planarity of the Pt coordination as indicated by the values of the displacement of the four N donors from the PtN_4 mean plane, not exceeding 0.1 Å (Table VIII). The bowing is probably due to the bite of 1-MeC$^-$, ranging from 2.29 to 2.36 Å in all the cations, shorter than the metal–metal distance. In fact, in the analogous cations $[(MeNH_2)_2PtL_2Hg]^{2+}$ (L = 1.5-Me_2C^- and 1-MeC$^-$), where the Pt–Hg distances are 2.764(1) and 2.785(1) Å, the N4–Hg–N4A angles are 164.1 and 163.2(2)°.[23] Furthermore, an increase of the tetrahedral distortion around Pt is observed, the corresponding displacement of the four N donors from the mean PtN_4 plane being ±0.14 and ±0.11 Å, respectively.

In **9b** and **12b**, the NH_2Me ligands are oriented with respect to the remaining nearly planar moiety of the cation in such a way that their methyl groups are on the oxygen side, nearly equidistant from O2 and O2A. This orientation appears to be determined by weak H bonds formed by N11 and N12 atoms with nitrate oxygens and the water molecules in both **9a** and **12a** (see next section). The torsional angles N3–Pt–N11–C11 and N3–Pt–N12–C12 range from 73(2) to 95(1)° (conformation A). The Pt–N–Me angles in **12b** are 113.5(9) and 114.0°. In contrast to complexes **9a** and **12a**, in both of the two above cited Pt,Hg analogues, one of the two NH_2Me ligands is rotated about the Pt–N12 bond by approximately 180° with respect to the conformation A (conformation B), with the Me group pointing toward Hg at mean Hg···CH_3 and Hg···HCH_2 distances of 3.4 and 2.6 Å, respectively.[23] In the latter cations, the Pt–N12–C12 and Hg–Pt–N12 angles widen to about 120 and 96°, respectively, while the Pt–N11–C11 and Hg–Pt–N11 angles are very close to those found in **12b**. The different geometry between the two $PtNH_2Me$ groupings in Pt,Hg complexes may be interpreted as due to the need either to relieve the interaction between Me and Hg or to adjust the orientation of the MeC–H bond with respect to Hg for improving an agostic[35] or a hydrogen bond[36] interaction. The orientation of NH_2CH_3 toward Hg may be determined by the involvement of N12, in contrast to N11, in two H bonds with the O atoms of another cation. Rotation about the Pt–N bonds from conformation A to B in **12b** leaving the Pt, Pd, N11, C11 and H atoms all coplanar, gave calculated Pd···CH_3 and Pd···HCH_2 contacts of 2.9 and 2.1 Å, respectively, with the methyl H atom nearly in the apical position of Pd (H–Pd–Pt and C–H–Pd angles of 74 and 151°, respectively (Figure 1)). After a rotation of 60° around the N11–C11 bond, the calculated Pd···H distance is 2.6 Å.

Crystal Packing. The crystal packing of all the compounds is built up by large cations, nitrate anions, and water molecules of crystallization, held together by electrostatic, hydrogen bond, and Van der Waals interactions. In **2a** and **6a**, a pair of *trans*-$[(NH_3)_2Pt(1\text{-}MeC^-)_2PdY]^+$ cations, arranged about a crystallographic symmetry center, are held together by hydrogen bonds between one NH_3 ligand of one cation and the O atoms, O2′ and O2A′, of the other and vice versa (N12···O2′ = 2.936(6) Å and N12···O2A′ = 2.868(6) Å, in **2a**, and N11···O2′ = 2.819(6) Å and N11···O2A′ = 2.873(6) Å in **6a**). Other contacts below 2.9 Å are OW1···O73 (2.792(6) Å) in **2a** and N11···OW3 (2.865(8) Å), O49···OW2 (2.846(7) Å), and O49···OW1 (2.687(7) Å) in **6a**. The cation arrangement in **4a** is related to those of **2a** and **6a**. However, within each pair of cations, arranged about the crystallographic symmetry center, two water molecules are inserted (OW1 and OW1′ related by the symmetry center). Therefore, each water molecule makes hydrogen bonds to N11 (2.956(6) Å) and to O2A (2.773(6) Å) of one cation and to O2′ (2.801(6) Å) of the other. In **9b**, the hydrogen bonds are O2···OW1 (2.74(2) Å), OW1···OW2 (2.80(2) Å), and O2A···OW2 (2.90(2) Å) in addition to contacts N11···O71 and N12···O71 of 2.84(2) and 2.95(2) Å, respectively. In **12b**, distances below 3 Å involve OW1, which bridges two cations through contacts of 2.84(2) Å with N12 of one cation and of 2.95(1) Å with O2A of the other.

Scheme I

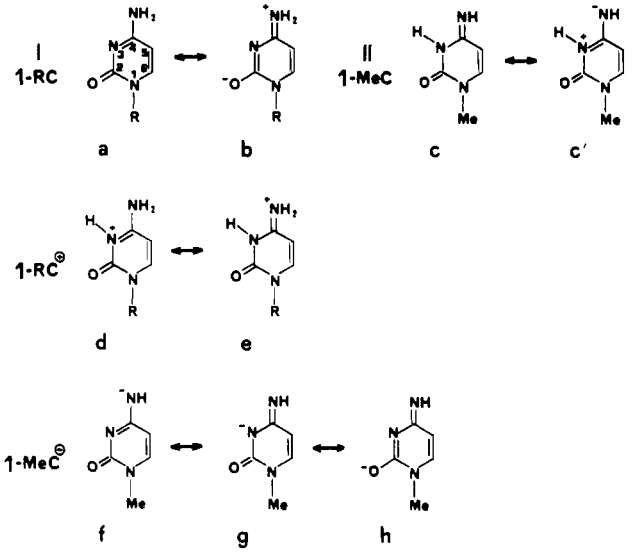

Geometry of the 1-MeC$^-$ Ligand. The molecular dimensions of neutral (**a**, Scheme I) and protonated (**d**, Scheme I) cytosine residues have been obtained by Taylor and Kennard averaging 17 and 14 residues, respectively by simple VBS theory.[53] Mean bond lengths and angles are reported in Table IX. The changes in C2-N3, C4-N3, C2-O2 and C4-N4 distances suggest that resonance forms **b** and **e** (Scheme I) are important in 1-RC and in 1-RC$^+$ residues, respectively, but **e** contributes to the 1-RC$^+$ residue more than **b** does in the neutral one. Furthermore, protonation leads the angles C2–N3–C4 and N3–C2–O2 to increase and the ring internal angles at C2 and C4 to decrease. The molecular dimensions of the uncoordinated 1-MeC (I, R = Me in Scheme I),[54] also given in Table IX, are in very good agreement with those of 1-RC. Analogously, the geometry of the imino–oxo tautomer II, coordinated through N4 to Pt,[55] is essentially equal within the experimental errors to that of 1-RC$^+$ and, therefore, the resonance form **c′** has a significant contribution. The geometry of the deprotonated 1-MeC$^-$, coordinated through N3 and N4 (1-MeC$^-$-*N3,N4*), was obtained averaging bond lengths and angles of the ligand in the structure **2a**, **4a**, and **6a** for which estimated standard deviations of C–C bond lengths were less than 0.01 Å. The mean values are given in Table IX together

(49) Sinn, E.; Flynn, C. M.; Martin, R. B. *Inorg. Chem.* **1977**, *16*, 2403.
(50) Davidson, J. L.; Preston, R. N.; Spankie, S. A. R.; Douglas, G.; Muir, K. W. *J. Chem. Soc., Dalton Trans.* **1989**, 497.
(51) To be published.
(52) Umakoshi, K.; Ichimura, A.; Kinoshita, I.; Ooi, S. *Inorg. Chem.* **1990**, *29*, 4005.
(53) Taylor, R.; Kennard, O. *J. Mol. Struct.* **1982**, *78*, 1.
(54) Rossi, M.; Kistenmacher, T. J. *Acta Crystallogr.* **1977**, *B33*, 3962.
(55) Lippert, B.; Schöllhorn, H.; Thewalt, U. *J. Am. Chem. Soc.* **1986**, *108*, 6616.

Table IX. Comparison of (1-MeC⁻-*N3,N4*) Ligand Geometries with Those of the Protonated (1-RC⁺) and Neutral Residues (1-RC) of Cytosine and of Uncoordinated Cytosine (1-MeC) with the Mean Values of (1-MeC-*N3*) Also Reported

	1-RC⁺ [a]	1-RC[a]	1-MeC[b]	1-MeC⁻-*N3,N4*[c]	1-MeC-*N3*[d]
			Distances (Å)		
N1–C1			1.464(2)	1.466(5)	1.469(1)
N1–C2	1.381(2)	1.399(4)	1.395(2)	1.380(6)	1.380(2)
C2–N3	1.387(2)	1.356(3)	1.358(2)	1.367(8)	1.375(3)
N3–C4	1.352(2)	1.334(2)	1.332(4)	1.372(5)	1.348(1)
C4–C5	1.413(2)	1.426(4)	1.422(2)	1.434(3)	1.408(1)
C5–C6	1.341(3)	1.337(2)	1.334(2)	1.330(5)	1.341(1)
C6–N1	1.362(2)	1.364(2)	1.357(2)	1.371(8)	1.355(3)
C2–O2	1.211(2)	1.237(2)	1.234(2)	1.222(3)	1.227(2)
C4–N4	1.313(2)	1.337(4)	1.336(2)	1.307(5)	1.329(1)
			Angles (deg)		
C6–N1–C2	121.5(1)	120.6(1)	120.1(1)	120.8(4)	120.7(2)
N1–C2–N3	114.9(2)	118.9(2)	118.0(1)	117.7(4)	117.2(2)
C2–N3–C4	125.1(2)	120.0(2)	120.0(1)	122.9(3)	121.3(1)
N4–C4–C5	117.5(2)	121.8(2)	121.8(1)	117.9(3)	120.4(1)
C4–C5–C6	118.5(1)	117.6(2)	117.2(1)	119.2(3)	118.1(1)
C5–C6–N1	122.5(1)	121.0(2)	121.8(1)	122.0(2)	121.4(1)
N1–C2–O2	123.5(2)	119.2(2)	118.6(1)	121.4(4)	120.9(3)
N3–C2–O2	121.6(1)	121.9(2)	122.4(1)	120.9(5)	121.9(1)
N3–C4–N4	119.5(2)	117.9(2)	117.8(1)	119.2(2)	118.7(2)
C5–C4–N4	123.0(3)	120.3(2)	120.1(1)	123.4(3)	121.0(3)
C2–N1–C1			118.5(1)	120.7(2)	121.5(3)
C6–N1–C1			121.5(1)	118.7(4)	117.8(1)

[a] Reference 53. [b] Reference 54. [c] Mean values and esd of the mean from structures **2a**, **4a**, and **6a** ($n = 6$). [d] Mean values and esd of the mean of three structures with σ(C–C bond) less than 0.01 Å, namely: *trans*-Pd(1-MeC-*N3*)$_2$Cl$_2$,[49] *trans*-[Pd(1-MeC-*N3,N4*)$_2$(NH$_3$)$_2$](NO$_3$)$_2$,[15] and *cis*-[Pt(tmeda)(1-MeC-*N3*)Cl]ClO$_4$ (tmeda = *N,N,N',N'*-tetramethylethylenediamine).[67]

with those averaging data from three structural determinations, of the neutral 1-methylcytosine coordinated through N3 (1-MeC-*N3*). The changes in bond lengths of 1-MeC⁻ with respect to the neutral and protonated species indicate that resonance from **h** should contribute significantly in addition to forms **f** and **g**. This is consistent with the lengthening of the C4–N3 bond and the shortening of the C4–N4 one with respect to the neutral ligand, although there should be some additional influences, also due to the coordination that are difficult to rationalize. Bond angles appear to be intermediate between those of 1-RC and 1-RC⁺. Finally, in the neutral (1-MeC-*N3*) ligand, bond lengths involving N3, are modified with respect to those of the free ligand and approach those of 1-RC⁺. The above results suggest that the neutral, protonated, and deprotonated 1-RC ligands have significantly different geometries, which in turn appear to be affected by coordination to metals.

Discussion

Bonding Situation. The dinuclear PtPd cytosinyl complexes described in this work are of a type previously not observed in dinuclear nucleobase compounds of Pt and/or Pd. In the latter cases the two metals are either too far apart to have any interaction through space, e.g. in Pt$_2$(purine-*N7,N1*),[56] or they approach each other via their $nd_{z^2}/(n+1)p_z$ orbitals with the two metal coordination planes more or less parallel.[9,13b,20] In the compounds reported here, the metal coordination planes are at right angles to each other and the two metals form a strong bond. In unbridged Pt^{I}Pd^{I} compounds,[57] the metal coordination planes are likewise almost perpendicular, but relative orientations of the metal orbitals are different in the two systems (Chart II). Pt-Pd bond formation

Chart II

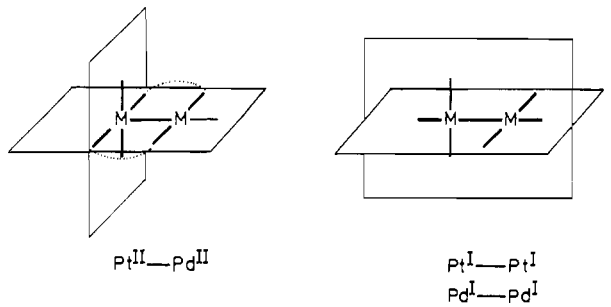

in our compounds is immediately evident from the fact that Pt^{II} is a ligand of Pd^{II}, which otherwise would be three-coordinate only. The shortness of the Pt–Pd distances (2.492(3)–2.521(1) Å) agrees with this view, even though it is not by itself a sufficient argument for metal–metal bond formation: There are several examples of dinuclear, μ-hydroxopyridonato-bridged Pd^{II} complexes with short (2.55–2.57 Å) Pd^{II}–Pd^{II} separations, yet with a formal bond order of zero.[58] Intermetallic distances as observed in PtPdY are in the range of Pt^{I}Pt^{I} and Pd^{I}Pd^{I} compounds (2.60–2.53 Å),[57] of the cyclic, tetranuclear μ-acetato complexes of Pt^{II} (ca. 2.49 Å),[59] and in the lower range of diplatinum(III) compounds (2.45–2.61 Å).[8]

The metal-metal bond in our compounds may be described by a Pt^{II} → Pd^{II} dative bond formalism,[60] resulting from the overlap of a filled d_{z^2}-like MO of Pt with an empty $d_{x^2-y^2}$-like orbital of Pd. An alternative description as a covalent Pt^{III}-Pd^{I} bond is inconsistent with (i) the Pt–Pd bond length being hardly affected by Y (maximum difference between μ-pyz compound **9b** and SCN compound **12b** is 0.029 Å) and (ii) the absence of any apparent trans influence of the Pt–Pd bond on the Pd–Y distances. The latter are close to distances observed in mononuclear PdY compounds. The N,N bite distance of the bridging 1-MeC⁻ ligand appears not to be primarily responsible for the shortness of the Pt–Pd bond, considering the structurally similar PtHg and PtAg compounds, which have substantially longer metal–metal separations.[23] We do not wish to rule out a situation, with an appropriate ligand Y, that could be better described by a Pt^{III}–Pd^{I} bond rather than the Pt^{II}→Pd^{II} formalism. As demonstrated by Fackler et al. in dinuclear Au and mixed Au$_2$Pt compounds, suitable axial ligands may influence the degree of metal–metal bond formation considerably.[61] There appears to be even the possibility that metal–metal-bonded compounds exist in two isomeric forms, to be described formally by a dative *and* a covalent metal–metal bond formalism,[62] and that the two isomers are in dynamic exchange with individual isomers stabilized to different degrees by the solvent.[63]

^{195}Pt NMR spectroscopy proved to be a method more sensitive towards variations of Y in PtPdY than X-ray crystallography. Chemical shifts of halide complexes *trans*-[(CH$_3$NH$_2$)$_2$-Pt(1-MeC⁻)$_2$PdY]⁺, prepared in situ from **3b** by adding an excess of halide, display a nearly linear dependence from electronegativity

(56) See, e.g.: (a) Frommer, G.; Schöllhorn, H.; Thewalt, U.; Lippert, B. *Inorg. Chem.* **1990**, *29*, 1417. (b) Lock, C. J. L.; Speranzini, R. A.; Turner, G.; Powell, J. *J. Am. Chem. Soc.* **1976**, *98*, 7865.
(57) (a) Usón, R.; Forniés, J.; Espinet, P.; Fortuno, C.; Tomás, M.; Welch, A. J. *J. Chem. Soc., Dalton Trans.* **1989**, 1583. (b) Rutherford, N. M.; Olmstead, M. M.; Balch, A. L. *Inorg. Chem.* **1984**, *23*, 2833.
(58) (a) Clegg, W.; Garner, C. D.; Al-Samman, M. H. *Inorg. Chem.* **1982**, *21*, 1897. (b) Bancroft, D. P.; Cotton, F. A.; Falvello, L. R.; Schwotzer, W. *Inorg. Chem.* **1986**, *25*, 1015.
(59) (a) Yamaguchi, T.; Sasaki, Y.; Nagasawa, A.; Ito, T.; Koga, N.; Morokuma, K. *Inorg. Chem.* **1989**, *28*, 4312. (b) Corrondo, M. A. A. de C. T.; Skapski, A. C. *J. Chem. Soc., Chem. Commun.* **1976**, 410; *Acta Crystallogr.* **1978**, *B34*, 1857, 3576.
(60) For other heteronuclear compounds interpreted in dative bond terms (donor–acceptor metal–metal bond), see e.g.: (a) Mc Donald, R.; Cowie, M. *Inorg. Chem.* **1990**, *29*, 1564. (b) Usón, R.; Forniés, J.; Tomás, M.; Ara, I.; Casas, J. M.; Martin, A. *J. Chem. Soc., Dalton Trans.* **1991**, 2253. (c) Liston, D. J.; Ja Lee, Y.; Scheidt, W. R.; Reed, C. A. *J. Am. Chem. Soc.* **1989**, *111*, 6643. (d) Batchelor, R. J.; Davis, H. B.; Einstein, F. W. B.; Pomeroy, R. K. *J. Am. Chem. Soc.* **1990**, *112*, 2036.
(61) King, C.; Heinrich, D. D.; Garzon, G.; Wang, J.-C.; Fackler, J. P., Jr. *J. Am. Chem. Soc.* **1989**, *111*, 2300.
(62) Einstein, F. W. B.; Jennings, M. C.; Krentz, R.; Pomeroy, R. K.; Rushman, R.; Willis, A. C. *Inorg. Chem.* **1987**, *26*, 1341.
(63) Ni, J.; Kubiak, C. P. *Inorg. Chem.* **1990**, *29*, 4345.

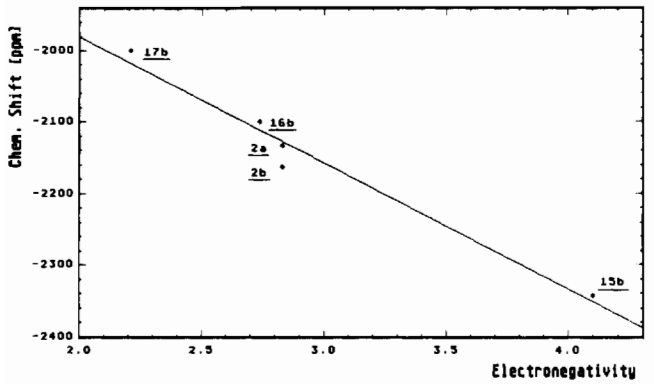

Figure 8. ^{195}Pt NMR chemical shifts of PtPdY with Y = F^-, Cl^-, Br^-, and I^- and their dependence on electronegativity (Allred–Rochow).

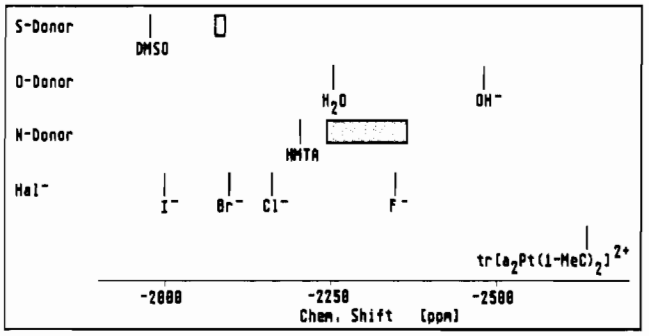

Figure 9. ^{195}Pt NMR chemical shifts of *trans*-$[a_2Pt(1\text{-}MeC)_2]^{2+}$ and various *trans*-$[a_2Pt(1\text{-}MeC^-)_2PdY]^{n+}$ compounds (a = CH_3NH_2). Shifts of S donors (except Me_2SO) and N donors (except hmta) are not listed individually.

(Allred–Rochow scale) as shown in Figure 8. As expected, no simple relationship emerges when ^{195}Pt NMR chemical shifts of all the other Y groups are included (Figure 9).

Steric Aspects. As already pointed out in the Introduction, it appears that steric interference between the two trans-oriented amine ligands of Pt and any trans-oriented ligands of Pd(NH_3 or Cl^-) prevents formation of complexes of type *trans*-$[a_2Pt(1\text{-}MeC^-)_2PdY_2]^{n+}$ (n = 2 or 0) (Figure 10). With Y = NH_3, for example, the distance between Y and N of Pt-NH_2R would essentially correspond to the PtPd distance. While a torsion about the PtPd vector could relieve the steric clash between Y and NH_2R, it at the same time would shorten the Pt–Pd distance further. Other alternatives—change in coordination geometries of both metals toward tetrahedral or escape toward an A-frame structure (μ-amide bridging or NH_2R substitution by a μ-Y ligand)—are not realized. A comparison of distances between NH_3 ligands of two metal planes in dinuclear, μ-nucleobase complexes (1-MeU, 1-MeT, 1-MeC^-) of *cis*-$(NH_3)_2M$ (M = Pt^{II},Pd^{II},Pt^{III}) reveals that, even with a Pt–Pt distance as short as 2.560 Å, the shortest $NH_3\cdots NH_3$ separation is still 3.4 Å. The tilting of the metal coordination planes in all these cis compounds avoids any steric clash. In a hypothetical *trans*-$[(NH_2R)_2Pt(1\text{-}MeC^-)_2Pd(NH_3)_2]^{2+}$ compound, an unacceptably short interamine distance of well below 3 Å would have to be realized. Similar arguments apply to a hypothetical species *trans*-$(NH_2R)_2Pt(1\text{-}MeC^-)_2PdCl_2$, even though the interaction between Cl^- and amine protons might be attractive. In *cis*-$(NH_3)_2$-$Pt(1\text{-}MeT)_2PtCl_2$, $NH_3\cdots Cl$ separations of the two metal coordination planes are 3.47 and 3.51 Å, at a Pt···Pt distances of 2.861(1) Å.[64]

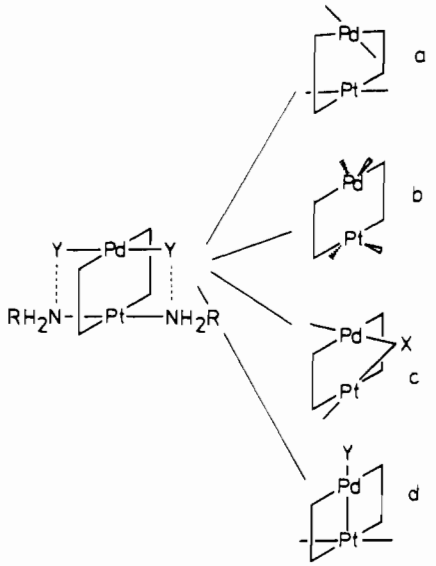

Figure 10. Hypothetical *trans*-$[(NH_2R)_2Pt(1\text{-}MeC^-)_2PdY_2]^{n+}$ compound with steric clash between Y and NH_2R ligands and four possible ways to escape this situation: (a) via torsion about the Pt···Pd vector, (b) via distortion toward tetrahedral geometries of the metals, (c) via formation of an A-frame structure with X = Y or X = NHR^-, (d) via loss of Y and Pt–Pd bond formation.

Axially Bound Nucleobases. Our studies on the interaction of $PtPd(H_2O)$ with nucleobases Y demonstrate the high reactivity of this entity toward nucleobases. Whether linking Pd^{II} to Pt^{II} changes the well-established binding patterns, the kinetics, and the preference of monomeric Pd^{II} electrophiles for nucleobase sites[22] needs to be studied further. While a few examples of nucleobase adducts with metal–metal bonded $[Pt^{III}]_2$[8d,65] and $[Rh^{II}]_2$[66] have been reported, the full scope and potential of dimetal entities binding to nucleic acids has never been explored. The same applies to reactions of such species with proteins and their potential applications as stains.

Note Added in Proof. After submission of this paper, an organometallic diplatinum complex with a dative Pt→Pt bond has been reported by M. Lin et al. (*J. Am. Chem. Soc.* **1992**, *114*, 4687).

Acknowledgment. This work was supported by the Deutsche Forschungsgemeinschaft, the Fonds der Chemischen Industrie and MURST, Rome Italy. We thank Mrs. Iris Dieter-Wurm for the preparation of **1b**, Mrs. Annette Danzmann for recording NMR spectra, Dr. Trevor G. Appleton for helpful discussions, and Asta Pharma (Frankfurt) for a loan of K_2PtCl_4.

Supplementary Material Available: Tables of complete crystallographic data, bond lengths and angles, thermal parameters, and hydrogen atom coordinates for **9b** and **12b**, a table of ^1H and ^{195}Pt NMR chemical shifts, and figures showing ^1H NMR spectra of **2a**, **2b**, and **5b** and an IR spectrum of **2b** (15 pages). Ordering information is given on any current masthead page.

(64) Micklitz, W.; Renn, O.; Schöllhorn, H.; Thewalt, U.; Lippert, B. *Inorg. Chem.* **1990**, *29*, 1836.
(65) El-Mehdawi, R.; Fronczek, F. R.; Roundhill, D. M. *Inorg. Chem.* **1986**, *25*, 3714.
(66) Rubin, J. R.; Haromy, T. P.; Sundaralingam, M. *Acta Crystallogr.* **1991**, *C47*, 1712.
(67) Preut, H.; Frommer, G.; Lippert, B. *Acta Crystallogr.* **1990**, *C46*, 1326.